Aust. J. Phys., 1985, **38**, 371–404

Theoretical and Experimental Techniques for the Determination of X-ray Anomalous Dispersion Corrections*

Dudley Creagh

Department of Physics, Faculty of Military Studies,
University of New South Wales, Royal Military College,
Duntroon, A.C.T. 2600.

Abstract

Theoretical and experimental techniques for the determination of the X-ray anomalous dispersion corrections $f'(\omega, \Delta)$ and $f''(\omega, \Delta)$ are discussed. The results of experiments on metallic, ionic and covalently bonded materials typified by copper and nickel, lithium fluoride, and silicon respectively are compared with the theoretical predictions. Attention is drawn to deficiencies in both the experimental and the theoretical approaches.

1. Introduction

A knowledge of the anomalous dispersion corrections for X rays is necessary for the solution of a wide range of problems involving the diffraction of X rays. The intensity of a scattered X-ray beam at a given distance from the scatterer depends on the square of the scattering power of the atoms which comprise the scatterer. Hence deviations in scattering power of the atoms from their normal values have a very significant effect on the intensities observed in X-ray scattering experiments. The influence of this anomalous scattering is felt in all sectors of crystallography, ranging from the solution of the phase problem in the structural analysis of large organic crystals to the study of epitaxial growth of III–IV and II–VI compounds by X-ray topography. Anomalous scattering can be a hindrance to the interpretation of experimental results or it can be of great assistance, the latter being the case if accurate values of the anomalous dispersion corrections are known.

Although the quantum mechanical theory of anomalous dispersion was developed by Waller (1927), and a nonrelativistic theory based on hydrogen-like wavefunctions was later extended by Sugiura (1927) and Hönl (1933*a*, 1933*b*), the ability to test experimentally the predictions of these theoreticians has really existed only since 1960. Attempts had been made to measure the anomalous dispersion corrections by a number of techniques ranging from deviation from the exact Bragg angle of reflection (Senström 1919; Duane and Patterson 1920; Hjalmar 1920) to measurements of the angle of deviation by a prism (Bearden 1931, 1932; Larsson *et al.* 1924). All these experiments measured the refractive index of the material being investigated, and the difficulty of achieving accuracy in the measurement of the X-ray refractive index can

* Dedicated to Dr A. McL. Mathieson on the occasion of his 65th birthday.

0004-9506/85/030371$02.00

be judged by the fact that the X-ray refractive index differs from unity only by a few parts per million. Given the primitive experimental facilities available at the time it is not surprising that these experiments did not have sufficient precision to test the predictions made by theory.

The further development of quantum mechanics saw the development of new scattering formalisms and the development of relativistic Hartree–Fock–Slater models of the atom. Many theoreticians made contributions to these new ways of describing the scattering of photons by atoms. However, the most demonstrably significant contribution was that made by Cromer and Liberman (1970) who used the relativistic Hartree–Fock wavefunctions of Brysk and Zerby (1968) to construct tables of the anomalous dispersion correction which were later to become part of the standard reference work used by crystallographers (Ibers and Hamilton 1974). Measurements are usually compared with this theoretical data base. Stibius-Jensen (1979) later drew attention to some unnecessary simplifications of the theory and the new versions of Cromer's computer program contain this suggested correction term.

Most of these advances have occurred because of the enormous improvement in digital computing power which has occurred in the past twenty years. This in turn was a consequence of the ability to manufacture large crystals of almost perfect silicon. It was only after these crystals became available to experimentalists that the predictions of Ewald (1916) concerning the dynamical theory of X-ray diffraction were verified. Through an understanding of the dynamical theory of X-ray diffraction, experimenters were able to conceive of the notion that the symmetric Laue reflection from a lattice plane in a perfect crystal could be used to phase split an incident beam. From this notion came the X-ray interferometer (Bonse and Hart 1965, 1966). X-ray interferometers have been used to provide extremely precise measurements of the X-ray refractive index of materials, over a large wavelength range which often includes the K- or L-absorption edge.

However, other dynamical scattering devices exist. In an experiment paralleling the early deviation-of-a-prism experiments Deutsch and Hart (1984) have designed a monolithic double crystal spectrometer which promises to provide results which equal the X-ray interferometer in their precision.

The nonrelativistic quantum theory shows that a direct relation exists between the imaginary part of the anomalous dispersion correction and the linear attenuation coefficient μ_l. Also the real and imaginary parts of the dispersion are linked by the Kramers–Kronig integral equation. It would seem that measurement of μ_l for a number of wavelengths should lead to the determination of both the imaginary and the real parts of the anomalous dispersion correction. Parratt and Hempstead (1954) and later Cromer (1965) used power law approximations to observed sets of measurements of μ_l to determine the real and imaginary parts of the anomalous dispersion corrections. More recently other authors (Creagh 1975, 1977, 1980; Gerward *et al.* 1979; Fuoss *et al.* 1981; Henke *et al.* 1982; Dreier *et al.* 1984) have attempted to produce anomalous dispersion data from measurements of μ_l.

Other, less direct, techniques for the measurement of X-ray anomalous dispersion corrections exist. These have their origin in Bijvoet's (1951) observation that the intensity of scattering from lattice planes $\{hkl\}$ in non-centrosymmetric crystal structures is different from that of the $\{\bar{h}\bar{k}\bar{l}\}$ planes. This was a most significant observation and has great importance in the solution of the phase problem in crystallography. For structures where the positional parameters of the atoms are known the problem can

be changed around, the intensity ratio being used to determine information about the anomalous dispersion corrections. This approach has been used by Fukamachi and Hosoya (1975) and Fukamachi *et al.* (1977) to observe the polar crystals GaAs and GaP. More recently an isomorphous replacement technique has been used by Templeton *et al.* (1980). The extent to which these less direct techniques can be applied to determine the anomalous dispersion coefficients will be discussed later in Section 3.

In this paper a brief discussion of the several theories of the anomalous scattering of photons by atoms will be given in Section 2. Section 3 describes the techniques which are at present being used for the determination of the anomalous dispersion corrections. In Section 4 the experimental results are compared with theoretical predictions.

2. Theories Concerning the Anomalous Scattering of Photons by Isolated Atoms

(a) Classical Model

The concept of an *atomic scattering factor* is an integral part of X-ray scattering theory. It has its origin in the classical nonrelativistic electromagnetic theory. Although this aspect has been discussed thoroughly in a number of texts [see e.g. James (1955) and Warren (1969) and the review articles by Gavrila (1981) and Kissel and Pratt (1983)] a brief resumé of its more important notions will be given here because the proper assessment of modern theories and experimental techniques depends on a correct understanding of these earlier definitions.

The discussion commences with the scattering of an unpolarized electromagnetic wave by a *free electron.* In Fig. 1*a* the geometry of this scattering process is shown. For a free electron situated at the origin the fraction of the intensity of the wave scattered through an angle ϕ is

$$I/I_0 = (r_e/r)^2 \tfrac{1}{2}(1+\cos^2\phi), \tag{1}$$

where r_e is the classical radius of the electron and r is the distance measured along the scattering direction at which the intensity is measured. Implicit in the derivation of this equation is the assumption that the wavelength of the scattered radiation has been unmodified in the scattering process: elastic or Rayleigh scattering has occurred.

To consider the scattering of electromagnetic waves by the electrons bound to an atom one must assume that each electron scatters as an individual and the atomic scattering is the sum of each of these individual contributions. The *atomic scattering factor* f is defined as the intensity scattered by an atom at wavelength λ to the intensity scattered by a free electron at wavelength λ. Because the electrons are not localized in space but are in rapid motion about the nucleus the atomic scattering factor can be written in terms of the electron density ρ which exists a distance r from the nucleus. Also, because the size of the atom is comparable with the wavelength of the incident electromagnetic wave (as shown in Fig. 1*b*), an electron within the atom will scatter as though its scattering factor is

$$f = \int \{\exp(2\pi\,\mathrm{i}/\lambda)(\hat{k}_f - \hat{k}_i)\,.\,r\}\rho\,\mathrm{d}V\,. \tag{2}$$

Here $\hat{k}_f - \hat{k}_i$ is the change in direction of the wavevector of the electromagnetic wave.

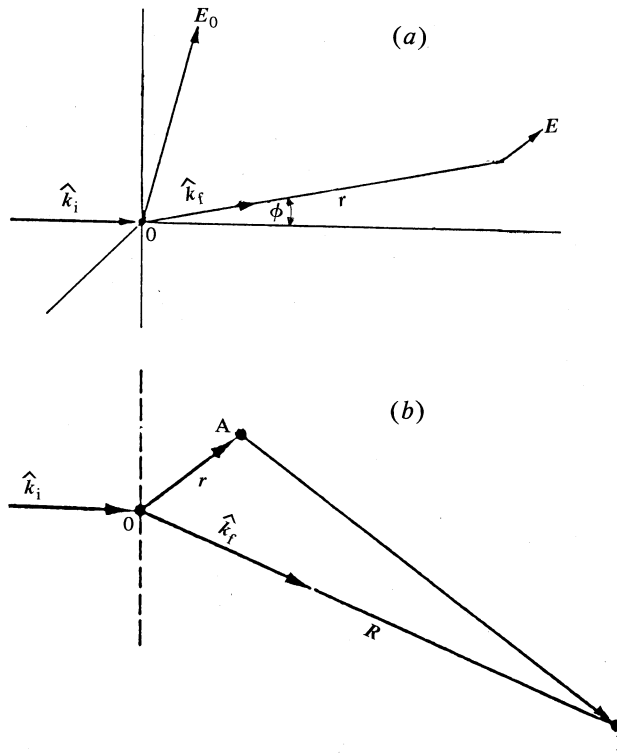

Fig. 1. Scattering by (*a*) a free electron situated at the origin 0 and (*b*) a bound electron situated at A. In (*b*) the pathlengths AP and 0P are different, leading to interference effects when the incident wavelength is comparable with the dimension of the atom.

The scattering factor f is the Fourier transform of the electronic charge distribution and is alternatively referred to as the *atomic form factor*.

If the atom is assumed to have a charge distribution with spherical symmetry equation (2) can be simplified, and

$$f = \int_0^\infty 4\pi r^2 \rho(r) \frac{\sin \alpha r}{\alpha r} \, \mathrm{d}r, \tag{3}$$

where $\rho = \rho(r)$, $\alpha = 4\pi \sin \theta/\lambda$ and $\theta = \frac{1}{2}\phi$. The assumption of spherical symmetry for the electron charge distribution is not unreasonable since the orbitals involved directly in the scattering processes are often closed shells and therefore have spherical symmetry. For an atom containing several electrons the atomic scattering factor becomes

$$f = \sum_n \int_0^\infty 4\pi r^2 \rho_n(r) \frac{\sin \alpha r}{\alpha r} \, \mathrm{d}r. \tag{4}$$

For forward scattering ($\theta = 0$) the value of $\sin(\alpha r)/\alpha r$ becomes unity and the scattering factor f becomes equal to Z, the total number of electrons in the atom. Hence,

we have

$$Z = \sum_n \int_0^\infty 4\pi r^2 \rho_n(r)\,\mathrm{d}r. \tag{5}$$

In general the radial distribution of electron density $\rho(r)$ must be known before f can be determined.

In the model most frequently used to explain the scattering of electromagnetic radiation by an electron bound to an atom the electron is considered to move about the nucleus with a characteristic angular frequency ω_n, and to be acted upon by a damping force proportional to the induced electron velocity when the electron is displaced from its natural path, given by $\kappa_n \mathrm{d}x/\mathrm{d}t$. Forced harmonic motion of the electron occurs and consequently it radiates as if it were a dipole radiator. When the displacement of the bound electron is compared with the displacement produced by the wave interacting with a single free electron, the following expression for the atomic scattering factor of the bound electron results:

$$f = \frac{\omega^2}{\omega^2 - \omega_n^2 - \mathrm{i}\kappa_n \omega}. \tag{6}$$

It is usual to extend this analysis to encompass a number of orbits, the angular frequencies of which may be written as $\omega_1, \omega_2, \ldots \omega_n$, for which there is a certain probability g_n for the electron to exist in the level having natural frequency ω_n. The real part of the scattering factor can then be rewritten as

$$\mathrm{Re}\,f = \sum_n \frac{g_n \omega^2}{\omega^2 - \omega_n^2} \quad \text{or} \quad \mathrm{Re}\,f = \sum_n g_n - \sum_n \frac{g_n \omega_n^2}{\omega_n^2 - \omega^2}. \tag{7a, b}$$

The probability g_n is referred to as the *oscillator strength* corresponding to the virtual oscillator having the natural frequency ω_n. Equation (7) takes the form

$$\mathrm{Re}\,f = f_0 + f', \tag{8}$$

where f_0 represents the sum of all the elements of the set of oscillator strengths and is therefore unity for the single electron atom considered earlier. The correction f' is referred to as the real part of the *anomalous dispersion correction.*

Because a large, effectively infinite number of oscillator states exist in an atom it is possible to rewrite the expression for f' (equation 7b) for an incident wave of angular frequency ω_i as

$$f' = \int_{\omega_n}^\infty \frac{\omega^2\,\mathrm{d}g/\mathrm{d}\omega}{\omega^2 - \omega_\mathrm{i}^2}\,\mathrm{d}\omega. \tag{9}$$

If the atom has k electrons each electron may be thought of as possessing its own oscillator density of states $(\mathrm{d}g/\mathrm{d}\omega)_k$, and the real part of the anomalous dispersion correction is the sum of the contributions of each of the k electrons:

$$f' = \sum_k \int_{\omega_k}^\infty \frac{\omega^2 (\mathrm{d}g/\mathrm{d}\omega)_k}{\omega^2 - \omega_\mathrm{i}^2}\,\mathrm{d}\omega. \tag{10}$$

The oscillator strength of the kth electron

$$g_k = \int_{\omega_k}^{\infty} \left(\frac{\mathrm{d}g}{\mathrm{d}\omega}\right)_k \mathrm{d}\omega \tag{11}$$

is in general different from unity but the total oscillator strength of the atom must be, by definition, equal to the total number of electrons Z in the atom.

The imaginary part of the anomalous dispersion correction f'' is linked to the attenuation of the wave by the medium through which it propagates. Consider a medium in which a density ρ of oscillator states of the same type exists. For this medium the dielectric susceptibility [defined by $\epsilon = \epsilon_0(1+\chi)$] can be deduced to be

$$\chi = -(\rho e^2/\epsilon_0\, m\omega^2)f\,. \tag{12}$$

The refractive index of the medium is given by

$$n = (1+\chi)^{\frac{1}{2}}, \tag{13}$$

and it must be remembered that n is complex since f is complex. A wave travelling in the $+z$ direction in a medium which commences at $z = 0$ will have an amplitude $\psi(z)$ given by

$$\psi(z) = \psi(0)\exp(\tfrac{1}{2}|k|\chi''z) \tag{14}$$

$$= \psi(0)\exp(-\mu_1 z), \tag{15}$$

where μ_1 is the linear attenuation coefficient. Note that the term 'attenuation' is used in preference to the widely used term 'absorption'. The decision to call the loss in beam intensity by scattering 'attenuation' was made (ICRU 1968) to avoid confusion with the dosimetry term 'absorption'.

Substituting for χ'' we have

$$\mu_1 = \frac{\rho e^2}{\epsilon_0\, m\omega c}\,\frac{\kappa_n\omega^2}{(\omega^2-\omega_n^2)^2+\kappa_n^2\omega_n^2}\,. \tag{16}$$

The atomic attenuation coefficient μ_a, the scattering power per virtual oscillator state, is

$$\mu_a = \frac{e^2}{\epsilon_0 m\omega c}\,\frac{\kappa_n\omega^2}{(\omega^2-\omega_n^2)^2+\kappa_n^2\omega_n^2}\,, \tag{17}$$

so that

$$f'' = (\epsilon_0\, m\omega c/e^2)\mu_a\,. \tag{18}$$

The atomic attenuation coefficient is related to the density of oscillator states by

$$\mu_a(\omega) = \frac{\pi^2}{2\epsilon_0\, mc}\,\frac{\mathrm{d}g}{\mathrm{d}\omega}, \tag{19}$$

and hence

$$f'' = \tfrac{1}{2}\pi\omega_i(\mathrm{d}g/\mathrm{d}\omega)_{k_i}\,. \tag{20}$$

Here $(\mathrm{d}g/\mathrm{d}\omega)_{k_i}$ is the density of oscillator states of the kth electron at frequency ω_i.

Whence an expression linking the real and the imaginary parts of the dispersion corrections can be written as

$$f' = \frac{2}{\pi} \sum_k \mathrm{P} \int_{\omega_k}^{\infty} \frac{\omega f''(\omega)}{\omega^2 - \omega_i^2} \, \mathrm{d}\omega, \tag{21}$$

where P represents the principal value of the integral over the range from ω_k to infinity. This integral, which links the real and imaginary parts of the dispersion correction, is referred to as a Kramers–Kronig integral. Note that the restoring force term involving κ_n has been omitted in equation (21).

Equations (19)–(21) are the fundamental equations of the classical theory of photon scattering and it is to these that all other theoretical results are compared. It is also important to remember that, although the concept of a medium or collection of atoms was introduced to give an explanation of the attenuation coefficient $\mu_a(\omega)$, these equations in reality apply only to spherical isolated atoms.

A similar situation exists for the nonrelativistic quantum mechanical theory to be discussed in Section 2*b* and the relativistic quantum theory discussed in Section 2*c*.

Referring to equations (13) and (16) one sees that f' can be determined *directly* by determining the refractive index of a medium and f'' can be determined *directly* by determination of the linear attenuation coefficient μ_l. Other less direct methods have made use of the dependence of f' and f'' on the local electron density function $\rho(r)$ within the medium. The results of these experiments will be compared in Section 4 with the results to be expected from theoretical calculations.

(b) Nonrelativistic Quantum Mechanical Models for Photon Scattering by Atoms

As in the classical theory the nonrelativistic quantum mechanical theories commence with the assumption that the photon interacts with a spherical free atom, and because we are here interested in elastic scattering only those interactions for which the internal energy of the atom remains invariant will be considered. It will also be assumed that the photon energy will be in the X-ray range so that only the electrons interact with the photons. The nuclear Thomson, nuclear resonance scattering and Delbrück scattering processes are neglected here; for review articles on these processes see, for example, Hayward *et al.* (1974) and Papatzacos and Mork (1975).

In the elastic scattering processes discussed here we have $|\boldsymbol{k}_i| = |\boldsymbol{k}_f|$, where $\boldsymbol{k}_i$ and $\boldsymbol{k}_f$ are the wavevectors of the incident and the scattered photons respectively. The scattering vector is $\boldsymbol{\Delta} = \boldsymbol{k}_i - \boldsymbol{k}_f$ and the scattering angle is denoted by ϕ. If it can be assumed that the atom has a rotationally symmetric electron cloud the Rayleigh scattering matrix element can be written as

$$M = M_1(\boldsymbol{e}_i \cdot \boldsymbol{e}_f^*) + M_2(\boldsymbol{e}_i \cdot \hat{\boldsymbol{k}}_f)(\boldsymbol{e}_f^* \cdot \hat{\boldsymbol{k}}_i), \tag{22}$$

where $\hat{\boldsymbol{k}}_i$ and $\hat{\boldsymbol{k}}_f$ are unit vectors in the directions of the wavevectors $\boldsymbol{k}_i$ and $\boldsymbol{k}_f$ respectively, and $\boldsymbol{e}_i$ and $\boldsymbol{e}_f$ represent the polarization of the photon. The amplitudes M_1 and M_2 depend now on ω and $\boldsymbol{\Delta}$. This matrix element depends on the state of polarization of the photons. The matrix element M_1 corresponds to a linear polarization state for which $\boldsymbol{e}_i$ and $\boldsymbol{e}_f$ lie perpendicular to the scattering plane.

In the classical case the incident and final polarizations were considered to be averaged. Here too an average is made over all polarization states and the differential

scattering cross section takes the form

$$\mathrm{d}\sigma/\mathrm{d}\Omega = \tfrac{1}{2} r_e^2(|M_1|^2+|M_2|^2). \tag{23}$$

In the photon–atom interaction the nucleus is assumed to be at rest at the origin and the interaction of the electrons of the atom with the radiation field for which the appropriate potential is $A(r, t)$ is considered. For this exposition, to emphasize the logical similarity to the classical case, the scattering by a one electron atom will be discussed. Generalization to the case of an n-electron atom can be effected by the inclusion of the appropriate summations over the number of electrons present in the atom.

The perturbed Hamiltonian for an atom containing one electron coupled to a radiation field having vector potential A (assuming that $\operatorname{div} A = 0$ and the scalar potential is zero) is given by

$$\hat{H} = \hat{H}_0 - \frac{e}{mc} A . P + \frac{e^2}{2mc^2} A^2, \tag{24}$$

where $\hat{H}_0$ is the Hamiltonian for the unperturbed atom and $P = \mathrm{i}\hbar\nabla$.

Applying second order perturbation theory one can obtain the matrix element for Rayleigh scattering of photons by an atom whose initial state is designated by 1. Following Akhiezer and Berestetskii (1957) one can write for the matrix element

$$\begin{aligned} M = {} & (e_1 . e_2^*) f_0(\Delta) \\ & + \frac{1}{m}\langle 1 | e_2^* P \exp(-\mathrm{i}\, k_2 . r) \frac{1}{\Omega_1 - \hat{H}_0} e_1 P \exp(\mathrm{i}\, k_1 . r) | 1\rangle \\ & + \frac{1}{m}\langle 1 | e_1 P \exp(\mathrm{i}\, k_1 . r) \frac{1}{\Omega_2 - \hat{H}_0} e_2^* P \exp(-\mathrm{i}\, k_2 . r) | 1\rangle, \end{aligned} \tag{25}$$

where e_1 and e_2 are the initial and final polarizations of the photon; $\Delta = k_2 - k_1$; $\hat{H}_0|1\rangle = E_1$, and $\Omega - \hat{H}_0$ is Green's operator associated to the Hamiltonian $\hat{H}_0$. Further, we have

$$\Omega_1 = E_1 + \hbar\omega + \mathrm{i}\,\xi, \qquad \Omega_2 = E_2 - \hbar\omega - \mathrm{i}\,\xi,$$

where ξ is an infinitesimal positive quantity. The first term in (25) corresponds to the atomic form factor and, for spherically symmetric states, has the form

$$f_0(\Delta) = \int_0^\infty \rho(r) \frac{\sin \Delta r}{\Delta r} r^2 \,\mathrm{d}r \tag{26}$$

and is identical to that predicted from classical scattering theory (equation 3).

For photon energies $\hbar\omega$ close to the resonance energy of an orbital the matrix element has a resonant behaviour due to the second and third terms of equation (25). These comprise the anomalous dispersion corrections. Note that the derivation of (25) does not contain any contribution to the scattering from radiation damping. More complete nonrelativistic treatments include terms to account for linewidths.

Extension to the case of an atom containing Z electrons is trivial (see e.g. Mizushima 1970), and involves only the incorporation of appropriate summations to the exposition given earlier. It is however convenient to adopt a different formalism to

describe the atomic scattering factor. Because we have been discussing the scattering of a photon with a change in momentum $\boldsymbol{\Delta}$ but not energy at a frequency ω, it is proper to write the atomic scattering factor as

$$f(\omega, \boldsymbol{\Delta}) = f_0(\boldsymbol{\Delta}) + f'(\omega, \boldsymbol{\Delta}) + \mathrm{i} f''(\omega, \boldsymbol{\Delta}), \tag{27}$$

where $f_0(\boldsymbol{\Delta})$ is the atomic form factor and $f'(\omega, \boldsymbol{\Delta})$ and $f''(\omega, \boldsymbol{\Delta})$ are respectively the real and the imaginary parts of the anomalous dispersion correction. In the dipolar approximation employed earlier it can be shown (Goldberger and Watson 1965) that, for forward scattering ($\boldsymbol{k}_\mathrm{i} = \boldsymbol{k}_\mathrm{f}$),

$$f'(\omega_\mathrm{i}, 0) = \frac{2}{\pi} \mathrm{P} \int_0^\infty \frac{\omega f''(\omega)}{\omega^2 - \omega_\mathrm{i}^2} \, \mathrm{d}\omega, \tag{28}$$

which may be compared with the classical equation (9) and, using the optical theorem (Gell-Mann *et al.* 1956),

$$f''(\omega, 0) = \frac{\omega}{4\pi r_\mathrm{e} c} \sigma_\mathrm{tot}(\omega). \tag{29}$$

Here $\sigma_\mathrm{tot}(\omega)$ is the total atomic scattering cross section, and this is to be compared with equation (18).

A particular extension of this nonrelativistic analysis of the scattering of photons by atoms is now discussed. Hydrogen-like wavefunctions were assumed for the electrons comprising the atom and appropriate shielding constants were introduced to account for inter-electron interactions. The technique was applied initially by Hönl (1933*a*, 1933*b*) to K-shell electrons and was later extended to the case of L-shell electrons by Eisenlohr and Muller (1954). A more modern exponent of this approach is Wagenfeld (1966, 1975, 1985).

Wagenfeld's use of the Bethe and Salpeter (1957) expression for the atomic photoelectric cross section and his use of hydrogen-like eigenfunctions [corrected for screening using Grodstein's (1957) screening constant] enabled a description of the scattering of a photon incident in the $+x$ direction, polarized in the y direction, by

$$\sigma = \frac{8 R^2 e^2 h^2}{m^2 c^2 k} \sum_{n', l', m'} \sum_{n, l, m} |\langle \rho' | (\partial/\partial y) \exp(\mathrm{i}\, k x) | \rho \rangle|^2. \tag{30}$$

The bra–ket notation is used here to represent the matrix element for the transition of an electron from a hydrogen-like eigenstate characterized by ρ, for which the quantum numbers are n, l, m, to an unbound state ρ' characterized by the quantum numbers of the ejected free electron.

Each shell contributes to the total cross section. For example, the contribution from the K shell $\sigma_{1\mathrm{s}}$ is calculated using the analytical form of the hydrogen-like eigenfunction $\psi_{1\mathrm{s}}$. The retardation factor within the matrix elements was expanded as a power series:

$$\exp(\mathrm{i}\boldsymbol{k} \cdot \boldsymbol{r}) = 1 + \mathrm{i}\, \boldsymbol{k} \cdot \boldsymbol{r} - \tfrac{1}{2}(\boldsymbol{k} \cdot \boldsymbol{r})^2 + \ldots. \tag{31}$$

The first term in this equation corresponds to the dipole approximation used earlier to determine the anomalous dispersion corrections. (The forced vibration of the electron was assumed to give rise to an electric dipolar radiation field.) The second and third terms correspond respectively to the electric quadrupole and mixed electric quadrupole

and mixed electric–dipole–octopole transitions. As Wagenfeld (1966) has shown these terms form part of a rapidly converging series for which analytic expressions can be obtained. From these values of the cross section the imaginary part $f''(\omega, 0)$ and the real part $f'(\omega, 0)$ can be calculated.

The attractive feature of this technique is that the wavefunctions have an analytical form. Other techniques, using self-consistent fields, require numerical solutions for the eigenfunctions and consequently demand access to large computer facilities. The technique is also able to predict values of $f'(\omega, \boldsymbol{\Delta})$ and $f''(\omega, \boldsymbol{\Delta})$: scattering in other than the forward direction can be considered. Knowledge of the form of the angular correction is of great importance to crystallographers involved in structure analysis since each diffracted beam corresponds to a nonzero value of $\boldsymbol{\Delta}$.

There are, however, inadequacies in this approach, the most serious being the assumption that each electron acts as though it is part of a hydrogen-like atom. The sole concession to electron–electron interaction is the inclusion of Grodstein's (1957) screening constant. Finally, the nonrelativistic basis for the theory must limit its usefulness to atoms with low atomic numbers.

In the final analysis it is how well theory and experiment agree with one another which determines the success or failure of a theory. The degree of success of the nonrelativistic quantum mechanical model used by Wagenfeld will be discussed in Section 4.

(c) Relativistic Quantum Mechanical Model for Scattering of Photons by Isolated Atoms

In the last 15 years considerable effort has been made by theoreticians to develop a relativistic quantum mechanical model for the scattering of photons by isolated atoms. For the most part, however, theoreticians have concentrated on calculations of cross sections of atoms such as uranium, lead and aluminium. Reference to this rather fragmented work is to be found in the review articles of Gavrila (1981) and Kissel and Pratt (1983). Three theoretical data sets are frequently referred to in papers. These are the tabulations of Storm and Israel (1970), Scofield (1973) and Cromer and Liberman (1970, 1981). Of these the latter forms the basis for tables of the anomalous dispersion corrections (Ibers and Hamilton 1974).

All commence with the description of the scattering of photons by bound electrons given by (Sakurai 1967)

$$S_{1\to 2} = 2\pi\,\mathrm{i}\,\delta(\mathscr{E}_1 + h\omega_1 - \mathscr{E}_2 - h\omega_2)\frac{2\pi r_e^2 h^2}{(\omega_1\,\omega_2)^{\frac{1}{2}}} f, \tag{32}$$

where

$$\begin{aligned} f = mc^2 \sum_{n^+}\Bigg(&\frac{\langle 2|\,\boldsymbol{e}_2\,.\,\hat{\boldsymbol{\alpha}}\,\exp(-\mathrm{i}\,\boldsymbol{k}_2\,.\,\boldsymbol{r})\,|\,n^+\rangle\langle n^+\,|\,\boldsymbol{e}_1\,.\,\hat{\boldsymbol{\alpha}}\exp(\mathrm{i}\,\boldsymbol{k}_1\,.\,\boldsymbol{r})\,|\,1\rangle}{\mathscr{E}_1 - \mathscr{E}_n^+ + h\omega_1} \\ &+ \frac{\langle 2|\,\boldsymbol{e}_1\,.\,\hat{\boldsymbol{\alpha}}\,\exp(\mathrm{i}\,\boldsymbol{k}_1\,.\,\boldsymbol{r})\,|\,n^+\rangle\langle n^+\,|\,\boldsymbol{e}_2\,.\,\hat{\boldsymbol{\alpha}}\,\exp(-\mathrm{i}\,\boldsymbol{k}_2\,.\,\boldsymbol{r})\,|\,1\rangle}{\mathscr{E}_1 - \mathscr{E}_n^+ - h\omega_2}\Bigg) \\ + mc^2 \sum_{n^-}\Bigg(&\frac{\langle 2|\,\boldsymbol{e}_2\,.\,\hat{\boldsymbol{\alpha}}\,\exp(-\mathrm{i}\,\boldsymbol{k}_2\,.\,\boldsymbol{r})\,|\,n^-\rangle\langle n^-\,|\,\boldsymbol{e}_1\,.\,\hat{\boldsymbol{\alpha}}\,\exp(\mathrm{i}\,\boldsymbol{k}_1\,.\,\boldsymbol{r})\,|\,1\rangle}{\mathscr{E}_1 - \mathscr{E}_n^- + h\omega_1} \\ &+ \frac{\langle 2|\,\boldsymbol{\epsilon}_1\,.\,\hat{\boldsymbol{\alpha}}\,\exp(\mathrm{i}\,\boldsymbol{k}_1\,.\,\boldsymbol{r})\,|\,n^-\rangle\langle n^-\,|\,\boldsymbol{e}_2\,.\,\hat{\boldsymbol{\alpha}}\,\exp(-\mathrm{i}\,\boldsymbol{k}_2\,.\,\boldsymbol{r})\,|\,1\rangle}{\mathscr{E}_1 - \mathscr{E}_n^- - h\omega_2}\Bigg). \end{aligned} \tag{33}$$

In (33) the usual bra–ket notation has been used to denote the matrix elements between energy states, 1 and 2 being respectively the initial and final states of the system, and n^+ and n^- being intermediate energy states of positive and negative energy respectively. The Dirac velocity operator $c\hat{\boldsymbol{\alpha}}$ operates on the retardation factors within the bra–ket. The summations are over all states of positive and negative energy not already occupied by electrons. Although this equation completely describes the scattering process it cannot be readily used and must therefore be manipulated into a more familiar form.

If one were to define an atomic scattering factor f_0 similar to f in equation (33), except that all the energy denominators are written as $2mc^2$ and the sums n^+ and n^- occur for all states without exception, then

$$f_0 = \frac{mc^2\langle 2|(\boldsymbol{e}_2 . \hat{\boldsymbol{\alpha}}\, \boldsymbol{e}_1 . \hat{\boldsymbol{\alpha}} + \boldsymbol{e}_1 . \hat{\boldsymbol{\alpha}}\, \boldsymbol{e}_2 . \hat{\boldsymbol{\alpha}}) \exp\{-\mathrm{i}(\boldsymbol{k}_1 - \boldsymbol{k}_2) . \boldsymbol{r})\}|1\rangle}{2mc^2} \tag{34}$$

$$= \boldsymbol{e}_1 . \boldsymbol{e}_2 \langle 2| \exp(\mathrm{i}\, \boldsymbol{\Delta} . \boldsymbol{r})|1\rangle, \tag{35}$$

which is identical in form to the nonrelativistic equation (26) for the atomic form factor.

The relativistic atomic scattering f may then be written as

$$f = f_0 + (f - f_0), \tag{36}$$

where $(f - f_0)$ is analogous to the anomalous scattering terms and is (usually) small compared with f_0. There will be contributions to $(f - f_0)$ from both positive and negative energy states and it is convenient to write

$$(f - f_0) = f^+ - f_0^+ + f^- - f_0^- . \tag{37}$$

The term f_0^+ corresponds to transitions similar to those in (35) but involving only transitions from the initial state to positive energy (unbound) states.

Using the dipole approximation and averaging over polarization, Cromer and Liberman (1970) showed that

$$f_0^+ = (2/3mc^2)\langle 1|\hat{p}^2/2m|1\rangle, \tag{38}$$

which, when summed over all the electrons, is equal to the total electronic kinetic energy E_0, which can be estimated using self-consistent field techniques.

The two terms involving the negative energy (bound) states can also be evaluated in a similar fashion, using the dipole approximation, and the three final terms of (37) can be written as

$$-f_0^+ + f^- - f_0^- = \tfrac{5}{3} E_0/mc^2, \tag{39}$$

which is a constant for a particular atom.

The principal anomalous scattering term f^+ is given by

$$f^+ = mc^2 \sum_{n^+} |\langle n^+|\boldsymbol{e} . \boldsymbol{\alpha} \exp(\mathrm{i}\, \boldsymbol{k} . \boldsymbol{r})|1\rangle|^2 \left(\frac{1}{\mathscr{E}_1 - \mathscr{E}_n^+ + \hbar\omega} + \frac{1}{\mathscr{E}_1 - \mathscr{E}_n^+ - \hbar\omega} \right). \tag{40}$$

Contributions from both occupied and continuum states are included in f^+. However,

the contribution due to unoccupied bound states is neglected because it is small compared with the value of f^+. A similar assumption was made for the nonrelativistic treatment of photon scattering. The summation over the continuum energy states $\mathscr{E}^+$ may be considered to be adequately represented by an integration over the continuum energy states.

A singularity exists in the first term in the denominator of (40) when $\mathscr{E}^+$ equals $\mathscr{E}+\hbar\omega$. Using the Cauchy principal value theorem, f^+ can be evaluated as

$$f^+ = mc^2\left(\mathrm{P}\int_{mc^2}^{\infty} \frac{2(\mathscr{E}^+-\mathscr{E}_1)|\langle\mathscr{E}^+|\,\boldsymbol{e}\,.\,\hat{\boldsymbol{\alpha}}\exp(\mathrm{i}\,\boldsymbol{k}\,.\,\boldsymbol{r})|1\rangle|^2}{(\hbar\omega)^2-(\mathscr{E}^+-\mathscr{E}_1)^2}\,\mathrm{d}\mathscr{E}^+\right)$$
$$+\mathrm{i}\,\pi\,mc^2|\langle\mathscr{E}^++\hbar\omega|\,\boldsymbol{e}\,.\,\hat{\boldsymbol{\alpha}}\exp(\mathrm{i}\,\boldsymbol{k}\,.\,\boldsymbol{r})|1\rangle|^2\,; \tag{41}$$

f^+ contains a real part which can be equated to $f'(\omega,0)$ and an imaginary part which can be equated to $f''(\omega,0)$.

Akhiezer and Berestetskii (1957) have shown that the photoelectric cross section at photon energy $\hbar\omega$ is given by

$$\sigma(\hbar\omega) = \frac{4\pi^2 e^2 m}{\omega c}\,mc^2|\langle\mathscr{E}_1+\hbar\omega|\,\boldsymbol{e}\,.\,\hat{\boldsymbol{\alpha}}\,\exp(\mathrm{i}\,\boldsymbol{k}\,.\,\boldsymbol{r})|1\rangle|^2\,. \tag{42}$$

Whence, we have

$$f''(\omega,0) = (1/4\pi r_{\mathrm{e}}\,c)\,\omega\sigma(\hbar\omega)\,, \tag{43}$$

which may be compared with equations (18) and (29). Evidently a one-to-one correspondence exists between the classical, the nonrelativistic and the relativistic formulae for the imaginary part of the dispersion correction at the level of approximation used, namely for forward scattering by isolated atoms and neglecting bound state contributions.

The real part of f^+ may be rewritten using the cross section $\sigma(\hbar\omega)\equiv\sigma(\mathscr{E}^+-\mathscr{E}_1)$:

$$\mathrm{Re}\,f^+ = \frac{1}{2\pi^2\hbar r_{\mathrm{e}}\,c}\,\mathrm{P}\int_{mc^2}^{\infty}\frac{(\mathscr{E}^+-\mathscr{E}_1)^2\sigma(\mathscr{E}^+-\mathscr{E}_1)\,\mathrm{d}\mathscr{E}^+}{(\hbar\omega)^2-(\mathscr{E}^+-\mathscr{E}_1)^2}\,. \tag{44}$$

This is identical in form to equation (21). It is *not*, however, equal to the real part of the dispersion correction $f'(\omega,0)$, and in this respect the relativistic approach differs from the other two. The term $-f_0^+ + f^- - f_0^-$ must be included so that

$$f'(\omega,0) = \mathrm{Re}\,f^+ + \tfrac{5}{3}E_0/mc^2\,. \tag{45}$$

In addition, the matrix element in the high energy limit for forward scattering without change in polarization is

$$f'(\infty,0) = \frac{5E_0}{3mc^2} + \frac{1}{2\pi^2\hbar r_{\mathrm{e}}\,c}\int_0^{\infty}\sigma(\mathscr{E}^+-\mathscr{E}_1)\,\mathrm{d}\mathscr{E}^+\,. \tag{46}$$

Rewritten in terms of oscillator strengths this is the relativistic form of the Thomas–Reiche–Kuhn rule which in the nonrelativistic case sums to Z, the total number of electrons in the atom. In the relativistic case the rule represents only the matrix element for forward scattering at infinite energy.

In the foregoing exposition a number of simplifications have been made, not the least of which was the extensive use of the dipole approximation to determine $-f_0^+ + f^- - f_0^-$, the term which depends on the total electron energy E_0. It has been pointed out by Stibius-Jensen (1979) that Cromer and Liberman (1970) employed the dipole approximation at an inappropriately early point in their argument, and that a further correction term equal to $\frac{1}{2}Z(\hbar\omega/mc^2)^2$ results if the dipole approximation is made later in the development of the theory.

To what extent do the photoelectric scattering cross sections of Cromer and Liberman agree with calculations by other authors, and also with experiment? Both the Cromer and Liberman (1970) and the Storm and Israel (1970) programs for computing the photoelectric scattering cross section have their origin in the Brysk and Zerby (1968) program designed to use relativistic Dirac–Slater wavefunctions. Where Cromer and Liberman differ from Storm and Israel is in the use of the Kohn and Sham (1965) rather than the Slater (1951) exchange potential. In addition they used experimental rather than computed eigenvalues. Scofield (1973) on the other hand employed a relativistic Hartree–Fock approach. Comparisons by Kissel *et al.* (1980) of the results of the several Dirac–Hartree–Fock–Slater calculations show that they predict cross sections in excellent agreement with one another despite their different origin and simplifying assumptions. Experimental evidence gained in the course of the International Union of Crystallography X-ray Attenuation Project by Creagh and Hubbell (1985) suggests that there exists no rational basis for preferring one data set to another. It would seem therefore that for most atoms the calculation of atomic photoelectric cross sections and therefore $f''(\omega, 0)$ to sufficient accuracy is purely a routine matter. Furthermore, using equation (44) and the appropriate correction terms, the calculation of $f'(\omega, 0)$ should become a routine procedure.

However, it must be stressed that both $f'(\omega, 0)$ and $f''(\omega, 0)$ have been calculated here only for the forward scattering case with no change in polarization. The extension to the more general case of a nonzero scattering vector $\boldsymbol{\Delta}$ is usually made using the assumption that the anomalous corrections have the same angular dependence as the form factor. However, Parker and Pratt (1982) have shown that this is not a realistic assumption and that a better approximation is that $f'(\omega, \boldsymbol{\Delta})$ and $f''(\omega, \boldsymbol{\Delta})$ are independent of angle. This conclusion must be compared with the predictions of Wagenfeld (1975) using the hydrogen-like model, which predicts a relatively simple dependence on scattering angle.

It must be further stressed that polarization changes in the scattering process have not been considered and that the state of polarization of the incident beam has a significant effect on the scattering cross section in the region of the absorption edge, as Templeton and Templeton (1985) have shown.

3. Experiments to Determine Anomalous Dispersion Corrections $f'(\omega, \boldsymbol{\Delta})$ and $f''(\omega, \boldsymbol{\Delta})$

(a) Theories and realities

In the foregoing sections the discussion has centred on the development of a theory for elastic scattering of photons by isolated spherical atoms. In reality, measurements are not made on isolated atoms but on condensed, usually crystalline, phases. Hence some comments must be made on the use of these theories to describe the scattering properties of crystalline materials.

Crystalline materials are characterized by a periodicity in electron density $\rho(\boldsymbol{r})$ within their structures and this periodicity can be described by a set of translation vectors $\boldsymbol{a}$, $\boldsymbol{b}$, $\boldsymbol{c}$ such that

$$\rho(\boldsymbol{r}) = \rho(\boldsymbol{r}+m\boldsymbol{a}+n\boldsymbol{b}+p\boldsymbol{c}), \tag{47}$$

where m, n, p are integers. This electron density is associated with the atoms which comprise the crystal structure. Within a unit cell whose volume is characterized by $V_c = \boldsymbol{a}.\boldsymbol{b}\times\boldsymbol{c}$, a number of atoms of different scattering powers may exist. If the position of the jth atom is u_j, v_j, w_j in units relative to the lengths of the translation vectors $|\boldsymbol{a}|$, $|\boldsymbol{b}|$, $|\boldsymbol{c}|$ then the scattering power of the unit cell is, for a Bragg reflection from the $\{hkl\}$ plane of the crystal, described by the *geometrical structure factor*

$$F_{hkl} = \sum_j f_j \exp\{2\pi\mathrm{i}(hu_j+kv_j+lw_j)\}. \tag{48}$$

In arriving at equation (48) the assumption has been made that each of the atoms scatters as though it were a spherical atom having an atomic scattering factor f_j. The crystal as a whole scatters like a lattice having translational periodicity given by the translation vectors $\boldsymbol{a}$, $\boldsymbol{b}$, $\boldsymbol{c}$ but with all the charge density localized on the lattice points and each lattice point scattering with a power F_{hkl} for the hkl Bragg reflection. The concept of the geometrical structure factor is central to many of the techniques to measure the anomalous dispersions corrections $f'(\omega, \boldsymbol{\Delta})$ and $f''(\omega, \boldsymbol{\Delta})$.

For experiments in which the forward scattering is measured no Bragg reflection occurs and $h, k, l \equiv 0,0,0$: the lattice scatters as the sum of the scattering powers of the individual atoms within the unit cell. For experiments involving diffraction the scattering vector $\boldsymbol{\Delta}$ becomes the reciprocal lattice vactor $\boldsymbol{g}_{hkl}$. Note that the analysis of the results of such experiments has inherent in it two unresolved theoretical difficulties: the assumption that each atom's spherical charge distribution is unaffected by the charge distributions of the other atoms within the crystal structure and, more importantly, the question of whether there exists a dependence of the anomalous dispersion corrections on angle.

In Section 2 it was shown that two macroscopic properties of a medium are related to the atomic scattering factor. These are the refractive index n and the linear attenuation coefficient μ_l. Both of these correspond to forward scattering of the photons by the medium and therefore enable a direct test of the theories of scattering. Remember that these theories were developed for the forward scattering case. Experiments to measure the X-ray refractive index will be discussed in Section 3*b*, while experimental techniques for the measurement of linear attenuation coefficient μ_l will be discussed in Section 3*c*. Those experiments which determine the anomalous dispersion corrections by the Bijvoet-pair and isomorphous replacement techniques will be discussed in Section 3*d*. Section 3*e* will suggest some other techniques which might be used to determine the anomalous dispersion corrections.

(b) Measurements of refractive index

Three techniques for measuring the X-ray refractive index of materials have evolved since 1960. The first is based on the use of X-ray interferometers, and the second and third are essentially revivals of the earlier techniques involving the measurement of deviation by a prism and angle of total external reflection.

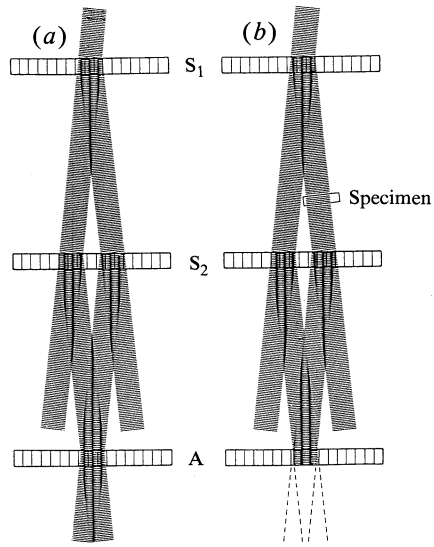

Fig. 2. X-ray interferometer where S_1, S_2 and A represent wafers of silicon and the lines represent Laue reflecting planes; S_1 and S_2 are phase splitters and A is the analysing wafer: (*a*) When the pathlengths are equal the standing wavefield lies between the Laue planes of A and the wave experiences little absorption.

(*b*) The insertion of a specimen into one of the beam paths shifts the phase of that beam and hence the position of the standing wavefield. The case shown here corresponds to the maximum of the standing wavefield falling upon the Laue planes where absorption is high.

X-ray Interferometer Measurements

The X-ray interferometer was invented by Bonse and Hart (1965). In the form most commonly used for refractive index measurement it is a device in which a boule of perfect single crystal silicon is cut to produce three wafers linked at the base and oriented so that the wafer surface is normal to the ⟨111⟩ direction and parallel to the ⟨220⟩ direction. As shown in Fig. 2 the thickness of the wafers is selected such that the intensities of the transmitted and reflected beam in the Laue reflection are equal, and the spacing between wafers is chosen to allow convergence of two of the beam paths at the surface of the third wafer. The X-ray beam undergoes Laue diffraction at each of the three wafers and is therefore referred to as an LLL interferometer. Because the two converging beams are phase coherent they interfere with one another producing a standing wave pattern in front of the third wafer. The position of this standing wavefield in relation to the Bragg reflecting planes of the third wafer determines the intensity of the beams transmitted through the wafer. If the wavefield maximum lies

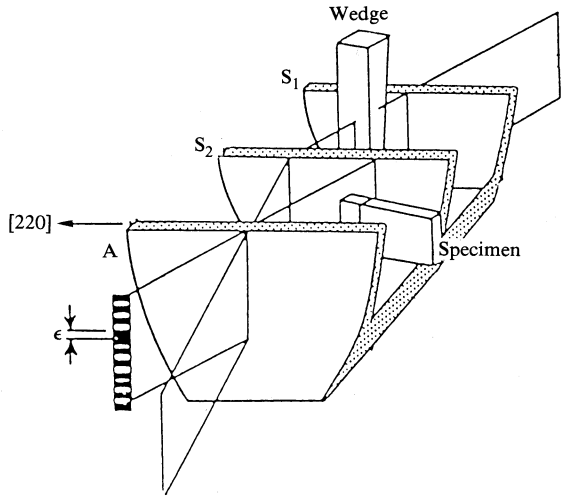

Fig. 3. Configuration used by Creagh (1968, 1970, 1975, 1980, 1984), Creagh and Hart (1970) and Bonse and Materlik (1975) to measure fringe shifts produced by a specimen placed in a beam path.

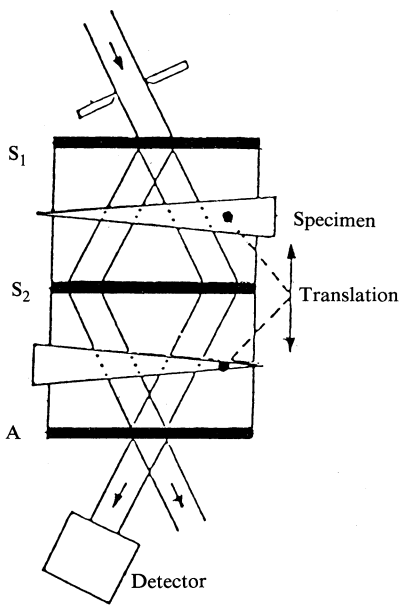

Fig. 4. Configuration used by Bonse and Hellkötter (1969). Translation of the wedges of specimen material causes the phase shift in the beam paths and hence variation in contrast in the beams.

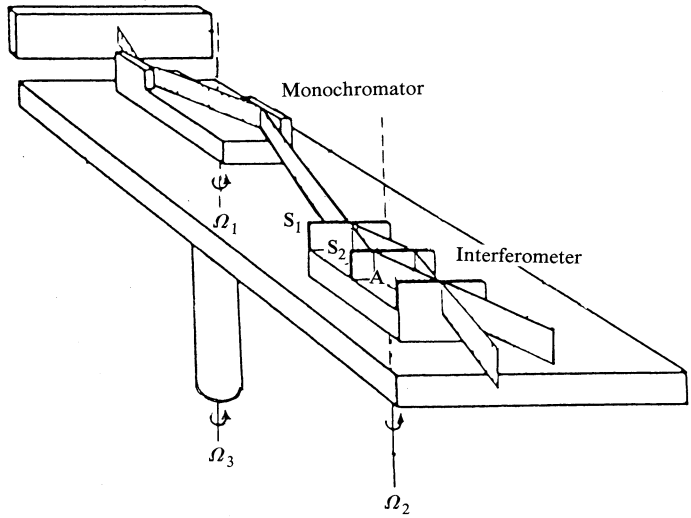

Fig. 5. Configuration used by Bonse and Materlik (1976) and Bonse *et al.* (1980, 1983). The X-ray beam from a synchrotron radiation source, made monochromatic by a double crystal monochromator, is incident upon the LLL interferometer. The monochromator and interferometer are turned by rotation about the axes Ω_1 and Ω_2 respectively. The interferometer system can be turned as a whole by rotation about the axis Ω_3.

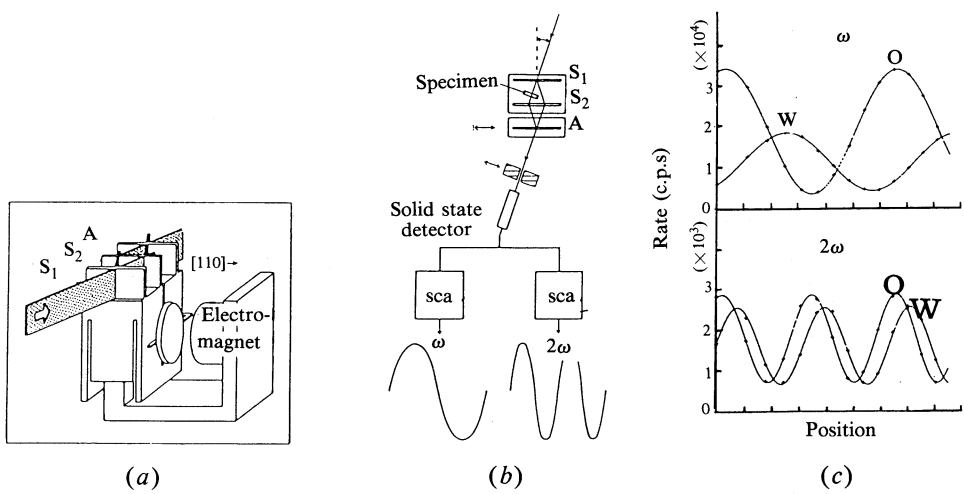

Fig. 6. (*a*) Schematic view of Hart's (1968) Ångström ruler showing the method of movement of the analysing wafer A, which is supported by leaf springs machined from the crystal. A magnetic force is used to displace the analysing wafer. (*b*) Configuration of the interferometer and the electronic system. Because a Bremsstrahlung source is used the fundamental (ω) and first (2ω) harmonic can be detected simultaneously by the solid state detector. As the wafer A is moved, contrast in the beam changes as the standing wavefield moves over the Laue reflecting planes. (*c*) Contrast variations with the motion of A with (W) and without (O) the specimen for both the fundamental (*top*) and the harmonic (*bottom*) radiations.

between the Bragg planes little energy is lost from the wavefield and a maximum of intensity is observed. If, however, the maximum of the standing wavefield lies on the Bragg plane the absorption of the beam is a maximum, and a minimum of intensity is seen in the transmitted beam. If an object is placed in one of the beam paths (Fig. 2*b*) it causes a shift in phase in that beam and therefore a shift in the position of the standing wavefield relative to the Bragg planes of the third wafer. A change in fringe pattern occurs. This phase shift is related directly to the X-ray refractive index by

$$p = (n - n_a)t/\lambda, \tag{49}$$

where n_a is the refractive index of air and t is the thickness of the object.

Various techniques have been used to enable this phase shift to be measured. Creagh (1968, 1970, 1975, 1980, 1984), Creagh and Hart (1970) and Bonse and Materlik (1972) inserted a lucite wedge into one beam path of an interferometer to provide fringes along the length of the reflected beam. The phase shift caused by inserting a parallel-sided specimen in the other path was measured using photographic techniques. This configuration is shown schematically in Fig. 3.

Bonse and Hellkötter (1969) used two wedges cut from the material under investigation, which were placed in the beam as shown in Fig. 4. Motion of the wedges across the beam caused the variation in optical path and this variation was recorded by means of an X-ray photon counting chain.

Bonse *et al.* (1983) used a technique reported by Bonse and Materlik (1976) and Bonse *et al.* (1980). In this technique a phase shifting plate was inserted into the beam as shown in Fig. 5 and the rotation of this plate about an axis perpendicular to the plane of reflection caused phase shifts, which were then detected by a solid state detector. Many of the experiments performed by Bonse's group have used radiation from the synchrotron at DESY, and very significant progress has been made in the precision of their experiments in the past five years. Indeed, in a recent paper Bonse and Hartmann-Lotsch (1984) claimed sufficient accuracy to confirm the mutual Kramers–Kronig relations which link $f'(\omega, 0)$ and $f''(\omega, 0)$; this implies an accuracy of better than one per cent.

All the other X-ray interferometer experiments have been performed using variations of Hart's (1968) Ångström ruler interferometer. This interferometer is manufactured such that its third wafer is linked to the block of silicon carrying the first two wafers by two silicon strips, as shown in Fig. 6*a*. By exerting a force on this wafer (either by means of an electromagnet or by capacitive coupling) the wafer itself can be made to move with respect to the standing wavefield. Without the specimen the wafer is driven to establish the standing wave pattern shown in Fig. 6*c* for monochromatic radiation. Variations in the transmitted beam intensity are detected using a solid state detector. Insertion of the specimen causes a phase shift, and a change in fringe contrast because of the attenuation of the beam in the specimen. This type of interferometer enables *direct* measurements of the refractive index n [and hence $f'(\omega, 0)$] and the linear attenuation coefficient μ_l [and hence $f''(\omega, 0)$].

All interferometers measure the X-ray refractive index by means of phase shifts (equation 49) and therefore measure a parameter which is directly related to the real part of the atomic scattering factor

$$n = 1 - \frac{r_e \lambda^2}{2\pi} \sum_j N_j f_j^r. \tag{50}$$

Here N_j is the number of atoms of type j per unit volume, and f_j^{r} is the real part of the atomic scattering factor in the forward direction. Writing 0 for $\boldsymbol{\Delta}$ in the form factor, since this is a case in which forward scattering occurs, we have

$$\mathrm{Re}\, f_j = f_j(0) + f_j'(\omega, 0). \tag{51}$$

If the normal crystallographic convention that $f_j(0)$ is equal to the total atomic number of the atom is followed, then we have

$$\mathrm{Re}\, f_j = Z_j + f_j'(\omega, 0). \tag{52}$$

The fringe shift at wavelength λ is given by

$$p_\lambda = r_e \lambda t \sum_j \{Z_j + f_j'(\omega, 0)\}/2\pi. \tag{53}$$

For both the Ångström ruler and the interferometer used by Bonse *et al.* (1983) the use of Bremsstrahlung radiation enables the detection of harmonics of the wavelength to which the interferometer was set simultaneously with the primary wavelength. These harmonics will exhibit different phase shifts from the primary wavelength since the refractive index depends on wavelength. The dominant harmonic wavelength is $\lambda/2$ and

$$p_{\lambda/2} = \tfrac{1}{2} r_e \lambda t \sum_j N_j \{Z_j + f_j'(2\omega, 0)\}/2\pi. \tag{54}$$

The ratio of these fringe shifts is therefore

$$P = p_\lambda / p_{\lambda/2} = 2 \sum_j \{Z_j + f_j'(\omega, 0)\} \Big/ \sum_j \{Z_j + f_j'(2\omega, 0)\}. \tag{55}$$

Note that this expression does *not* contain the specimen thickness. Since most recent measurements have been made in the region of an absorption edge, where $f'(\omega, 0)$ is a substantial fraction of Z_j and $f'(\omega, 0)$ is small with respect to Z_j, a simplification can be effected if the *theoretical* value of $f'(2\omega, 0)$ is used in equation (55). As Cusatis and Hart (1975) have shown the error in making this assumption is small compared with the error which occurs when the thickness of the specimen can be measured experimentally.

Using this technique it is possible to produce data at 2 eV intervals to 2% precision for an energy range which extends 1000 eV on both sides of the absorption edge (Hart and Siddons 1981). With such a device the various theoretical predictions of $f'(\omega, 0)$ and $f''(\omega, 0)$ can be put to the test.

Deviation of a Prism Experiment

In recent papers Deutsch and Hart (1984) have described a new double crystal diffractometer fabricated from a monolithic perfect crystal of silicon. The block is cut such that two wafers with Bragg planes hhh are oriented normal to the base block. A series of slits cut in the base block between the wafers form a folded leaf spring of the material between the wafers. Rotation of one wafer relative to the other is effected by bending the leaf spring by means of a small magnet attached to one segment and a small electromagnet attached to the other. A schematic diagram of the apparatus

is shown in Fig. 7. Notice that the reflections occur in the Laue case. Without the specimen (cut in the shape of a wedge) the rocking curve of a pair of *hhh* reflections can be measured. Because the crystals are perfect and have parallel sides the intensity of the main rocking curve is modulated by dynamical interference effects within the Bormann fan. Any of the modulation maxima would serve as an angle reference but in fact there exists a sharp central maximum, gaussian in shape, of 0·2 arc sec FWHM which is the most convenient reference point to use.

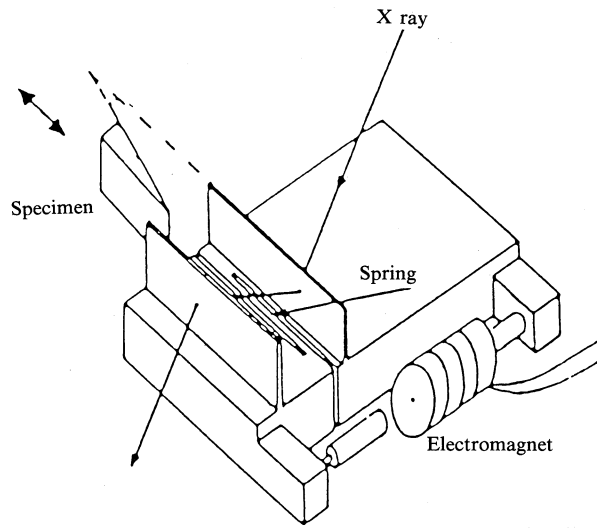

Fig. 7. Double crystal spectrometer by Deutsch and Hart (1984) for measurement of the deviation of the X-ray beam produced by a wedge-shaped specimen. The crystal wafers are linked by a spring machined from the single crystal silicon specimen. Rotation of one wafer with respect to another is done by changing the current in the electromagnet.

The insertion of a wedge in the beam between the two wafers causes the incident beam to deviate from exact Bragg reflection, and the second wafer can be rotated to return the second reflection to the peak of the rocking curve. Detection of the X-ray beam is by means of a solid state detector linked to a single channel pulse height analyser.

The effect of wedge angle is largely eliminated by using two related Bragg reflections, {777} and {888}, and measuring the deviations from exact Bragg reflection in each case. The angular conversion factor relating electromagnet current to angular rotation of the wafer is established by careful study of the rocking curve shapes and the comparison of these with the predictions of the dynamical theory of X-ray diffraction.

With this technique an accuracy of fractions of a part per billion is possible in measurements of the X-ray refractive index. Hence, $f'(\omega, 0)$ can be determined to a precision comparable with that of an X-ray interferometer.

Reflectivity Measurements

Perfect crystal techniques. The double crystal spectrometer used in the foregoing refractive index measurement was a Laue case (transmission) spectrometer. Double

crystal spectrometers can however be used in the Bragg case (reflection) to determine the real and imaginary parts of the anomalous dispersion correction.

The geometrical structure factor F_{hkl} is related to the integrated reflecting power of a perfect crystal for the Bragg case by the formula (Zachariasen 1945)

$$R_{\mathrm{H}}^{\theta} = \frac{P\lambda^2 r_{\mathrm{e}} |F'_{hkl}| \exp(-M)}{\pi |b|^{\frac{1}{2}} V \sin 2\theta_{\mathrm{B}}} R_{\mathrm{H}}^{\mathrm{y}}(g, k), \tag{56}$$

where P is the polarization factor, b is the ratio of the cosine of the incident to the cosine of the reflected angle of the beam (equal to 1 for symmetric reflection), V is the volume of the unit cell, θ_{B} is the angle of Bragg reflection, $R_{\mathrm{H}}^{\mathrm{y}}(g, k)$ is the Prins correction which corrects for absorption, and $\exp(-M)$ is the Debye–Waller factor.

The Prins correction is itself a complicated function. The parameters g and k are given by

$$g = -\frac{(1-b)V(1+k^2)^{\frac{1}{2}}}{4|b|^{\frac{1}{2}} r_{\mathrm{e}}\lambda |F_{hkl}| k \exp(-M)} \mu_{\mathrm{l}}, \tag{57}$$

$$k = F''_{hkl}/F'_{hkl}; \tag{58}$$

and

$$R_{\mathrm{H}}^{\mathrm{y}} = \int_{-\infty}^{\infty} \{L-(L^2-1)^{\frac{1}{2}}\} \, \mathrm{d}y, \tag{59}$$

where

$$L = y^2+g^2+\{(y^2-g^2-1+k^2)^2+4(gy-k)^2/(1+k^2)\}^{\frac{1}{2}}. \tag{60}$$

It is assumed that the parameters involved in this calculation such as the Debye–Waller factor, F''_{hkl} and P can be determined to sufficient accuracy, and use is made of accurate values of the integrand (59) computed elsewhere.

The technique is to measure the integrated reflectivity of a Bragg reflection, correct it for the influence of thermal diffuse and Compton scattering and then to compare it with the expression

$$\frac{P\lambda^2 r_{\mathrm{e}}}{\pi |b|^{\frac{1}{2}} \sin 2\theta_{\mathrm{B}}} R_{\mathrm{H}}^{\mathrm{y}}(g, k).$$

This had been computed using the best available values for the parameters involved in determining $R_{\mathrm{H}}^{\mathrm{y}}(g, k)$ and a suitable estimate of the polarization factor P. A value for $|F'_{hkl}| \exp(-M)$ results from which the real part of the anomalous dispersion correction may be deduced.

Freund (1975) has described an experiment to measure the integrated intensity of the 222 reflection from a nearly perfect crystal for a number of wavelengths in the vicinity of the K-shell absorption edge of copper. The copper crystal formed one element of the double crystal spectrometer, the other element being a (111) cut perfect crystal of silicon set to produce 333 reflections of the incident beam. Freund (1975) measured the linear attenuation coefficient μ_{l} directly. It is difficult, in the region of the absorption edge, to make such a definite measurement because of the existence of the extended X-ray absorption fine structure (EXAFS). Freund did not report the observation of EXAFS in this experiment, and further comment will be made on this in Section 4.

Using his data Freund (1975) produced values of the real part of the anomalous dispersion correction. These results however are not for $f'(\omega, 0)$ as in the earlier case,

but for $f'(\omega, g_{222})$, where $\boldsymbol{\Delta}$ the scattering vector is here set equal to the reciprocal lattice vector for the 222 Bragg reflection.

Total external reflection technique. The Laue case techniques mentioned earlier are unsuitable for use when the photon energy is low because the attenuation both of the measuring device and the sample itself becomes large. Consequently measurements become extremely difficult to make. If measurements have to be made in that region of the X-ray spectrum referred to as the vacuum ultra-violet, measurements of reflectivity would seem to be the most likely to provide reasonable results. The technique itself is based on Compton's (1923) observation that X rays are totally externally reflected by smooth surfaces. Note that this technique differs from that described in the previous subsection in that the scattering vector $\boldsymbol{\Delta}$ is not a reciprocal lattice vector. Henke *et al.* (1982) have shown that the reflection of an electromagnetic wave from a smooth (vacuum–material) interface can be described by a single complex constant and that, at the angle of total external reflection,

$$\sin^2 \theta_t + 2n - 2 = 0. \tag{61}$$

Measurement of θ_t allows direct calculation of the real part of the refractive index, provided absorption is not significant, and results in the determination of $f'(\omega, \boldsymbol{\Delta}_t)$, where $\boldsymbol{\Delta}_t$ is the scattering vector corresponding to the angle of total external reflection θ_t. A comprehensive compilation of low-energy X-ray interaction coefficients has been made by Henke *et al.* (1982) for Atomic Data and Nuclear Data Tables.

(c) X-ray attenuation techniques

It has already been shown in Section 2 that a direct relation exists between the imaginary part of the anomalous dispersion correction $f''(\omega, 0)$ and the linear attenuation coefficient μ_l. Attention has also been drawn to the fact that a Kramers–Kronig type of relation exists between $f''(\omega, 0)$ and the real part of the anomalous dispersion correction $f'(\omega, 0)$.

Indeed the semi-empirical theory of Parratt and Hempstead (1954) and the early work of Cromer (1965) made use of this inter-relationship. In both cases, however, power law fits were made to existing X-ray attenuation data originating in other laboratories and this simplified dependence of linear attenuation on photon energy was carried through in their calculations of $f'(\omega, 0)$.

The computer fitting of data acquired in X-ray attenuation measurements was employed by Creagh (1975, 1977, 1978, 1980) for the determination of $f'(\omega, 0)$ for alkali and alkaline-earth halides. A similar approach has been taken by Gerward *et al.* (1979) who determined $f'(\omega, 0)$ for silicon and germanium for a wide range of photon energies including, in the case of germanium, the K-shell absorption edge. Other determinations have been reported by Henke *et al.* (1982) for the interaction of low energy photons with a number of elements.

The advent of synchrotron radiation sources has stimulated much research interest in EXAFS and X-ray absorption near edge structure (XANES) because the high brilliance of these sources enables measurements to be made readily in those regions near the absorption edges where the linear attenuation coefficient is very large. Most of these measurements, however, have been of a qualitative, rather than absolute, nature. This follows from the deficiencies in the detectors used in the measurement

and also because the interpretation of EXAFS and XANES spectra has not required data which are correct on an absolute scale. Some efforts, however, have been made to place measurements on an absolute scale.

The use of the direct integration technique to determine $f'(\omega, 0)$ for germanium and selenium in the vicinity of the L_3 edges was described by Fuoss (1980) and Fuoss *et al.* (1981). A further summary of results was given by Fuoss and Bienenstock (1981).

More recently Dreier *et al.* (1984) have produced results for Ni, Cu, Zn and Zr close to their K edges, and Ta, W, Pt and Au near their respective L edges. Before giving details of their experiment a few comments concerning the measurement of linear attenuation coefficients must be made.

For 80 years attenuation data have been collected, and not an insignificant proportion of these data is inaccurate. The problem with the tabulated data was of such magnitude that the Commission on Crystallographic Apparatus of the International Union of Crystallography set up a project to determine which, if any, of the techniques for measuring μ_l could be trusted. In their report Creagh and Hubbell (1985) set out the criteria which must be met if reliable data are to be acquired. The experiments of Creagh and Gerward *et al.* met these criteria. Dreier *et al.* (1984), however, used a system whereby the relative data gained using standard EXAFS techniques were matched to X-ray cross sections tabulated by McMaster *et al.* (1969). During the fitting procedure a further energy dependent term had to be used to improve the quality of fit. When these data sets had been fitted to one another the direct integration technique was used. Because of the uncertainties in the McMaster *et al.* (1969) tables and the nature of the energy dependent term (which represents photon scattering processes that are not photoelectric in origin), there must be some significant uncertainties in their final results.

Finally, as Creagh (1980) has indicated, the Kramers–Kronig integration technique does not give the value of $f'(\omega, 0)$ if a relativistic quantum mechanical theory is used, and uncertainties must exist because of problems in calculating the correction terms using relativistic quantum mechanics.

(d) Diffracted intensity techniques

The intensity differences between inversion symmetry related diffracted beams from non-centrosymmetric crystals were first commented on by Bijvoet *et al.* (1951). All detection techniques determine the intensity rather than the amplitude and phase of a diffracted beam and this is related to $|F_{hkl}|^2$. For non-centrosymmetric structures one can write

$$I_{hkl}/I_{\bar{h}\bar{k}\bar{l}} = |F_{hkl}|^2/|F_{\bar{h}\bar{k}\bar{l}}|^2 . \tag{62}$$

This ratio contains terms for both $f'(\omega, g_{hkl})$ and $f''(\omega, g_{hkl})$ in both the numerator and the denominator except that the phase of the imaginary part for the inverted structure is opposite to the sign for the normal structure. Cole and Stemple (1962) studied the Bijvoet-pair reflections in the neighbourhood of the absorption edge and found that the ratio of intensities is independent of the defect state of the crystal and applies equally to ideally perfect as well as ideally imperfect crystals.

Fig. 8 shows schematically the relationship between Friedel pairs for a structure, where F_W is the scattering amplitude from atoms without dispersion and f' and

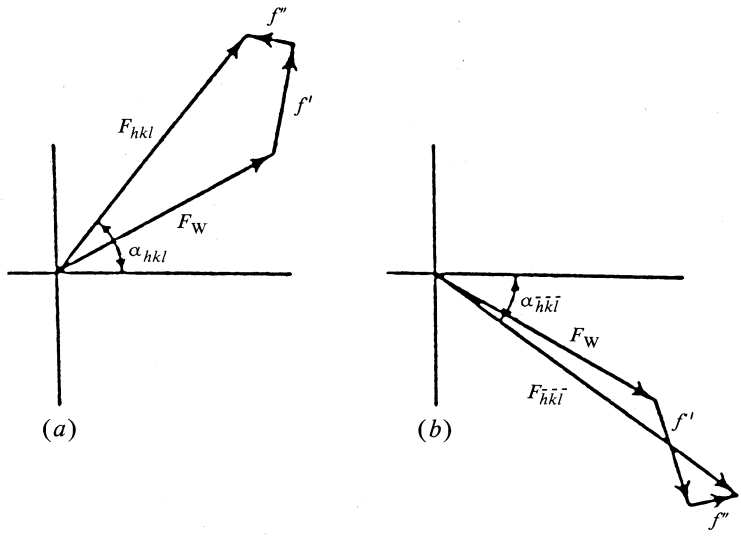

Fig. 8. Friedel pair scattering amplitudes and phases for (*a*) F_{hkl} and (*b*) $F_{\bar{h}\bar{k}\bar{l}}$. Note that $F_{hkl} \neq F_{\bar{h}\bar{k}\bar{l}}$ and $\alpha_{hkl} \neq -\alpha_{\bar{h}\bar{k}\bar{l}}$.

f'' are the resultants of scattering with dispersion from the atoms comprising the structure. Here we have

$$F_{hkl} = |F_{hkl}| \exp(\mathrm{i}\,\alpha_{hkl}), \tag{63}$$

where α_{hkl} is the phase angle. It is obvious that

$$F_{hkl} \neq F_{\bar{h}\bar{k}\bar{l}}, \qquad \alpha_{hkl} \neq -\alpha_{\bar{h}\bar{k}\bar{l}}. \tag{64}$$

Hosoya (1975) outlined several techniques for the determination of $f'(\omega, g_{hkl})$ and $f''(\omega, g_{hkl})$ from such measurements. In one technique the experimentally determined linear attenuation coefficient μ_l was used, from which values of $f''(\omega, g_{hkl})$ were deduced. Using this value $f'(\omega, g_{hkl})$ was calculated. In another technique, measurements on a set of Bijvoet pairs gave rise to a set of simultaneous equations, with $f'(\omega, g_{hkl})$ and $f''(\omega, g_{hkl})$ the solutions. Implicit in this, however, is the assumption that no angular dependence of anomalous dispersion corrections exists. This technique has been applied to studies of GaAs and GaP in the region of the gallium, arsenic and phosphide absorption edges by Fukamachi and Hosoya (1975) and Fukamachi *et al.* (1977, 1978). Other studies have been reported by Barnea (1975) for CdSe and by Post (1975) for ZnP, ZnS and BP. From his studies Post concludes: '... it would be more useful to base these (experimental tests of dispersion theory) on X-ray interferometric determinations of f' and careful measurements of the true photoelectric absorption cross sections, rather than measurements of the intensities of selected X-ray reflections.'

The problem can be approached from another angle. If the positions of all the atoms within a crystal structure have been determined its geometrical structure factor

F_{hkl} can be calculated to some precision. The relative intensities of each of the set of Bragg reflections for a particular photon energy can therefore be computed. If one then makes measurements at other photon energies the assumption could be made that the only parameter which changes is the scattering power of the atom. If the structure is then solved using the positional and thermal parameters determined previously the R factor will be different from that found earlier. Also, if one atomic species is near one of its absorption edges its anomalous scattering factors become dominant terms in the structure factor. This led Templeton and Templeton (1978) to refine the spectrum of caesium tartrate using the anomalous dispersion correction f'' as a free variable for photon energies in the neighbourhood of the caesium absorption edge. The success of this technique has led to a number of other measurements; see, for example, Philips *et al.* (1978), Templeton *et al.* (1980) and Philips and Hodgson (1980*a*, 1980*b*).

There are some problems inherent in this technique. The first is that it relies on the accurate measurement of the intensity of the diffracted beam and the conclusion by Cole and Stemple (1962) concerning the independence of intensity ratio on crystalline perfection. Other factors such as primary and secondary extinction also present difficulties to those making an accurate measurement of the intensities of the diffracted beams. A more serious flaw is its assumption that neither of the anomalous scattering corrections depends on the angle of scattering. By definition structure factor methods measure $f_j'(\omega, g_{hkl})$ and $f_j''(\omega, g_{hkl})$ for the atomic species j which is the major anomalous scatterer in the structure. Since it is not yet proven that no angular dependence of the anomalous dispersion correction exists this technique does not provide a good test of current theories.

Nevertheless, the concepts developed form the basis of an extremely powerful technique, the 'heavy atom' or isomorphous replacement technique, used to resolve the phase problem in the solution of complicated crystal structures. Discussions of these techniques are given in standard crystallographic texts, such as Stout and Jensen (1968).

Pendellösung Measurements

As Ewald (1916) showed there is an interchange in energy between the transmitted and the reflected beam propagating in a crystal structure. He called this phenomenon Pendellösung. The first observation of Pendellösung was by Kato and Lang (1959) in perfect crystals of silicon. The modern revival of the dynamical theory of X-ray diffraction commenced with the work of Kato (1960, 1961).

The intensity of the wavefield which results from the interference of the incident and diffracted beam is related to the geometrical structure factor by

$$I_{hkl} = A\pi^2 \Delta_0^{-2} \operatorname{cosec}^2\theta \{J_0(\pi l \Delta_0^{-1})\}^2, \tag{65}$$

where A is a constant and

$$\Delta_0 = \lambda \cos \theta / P|\chi_{hkl}|. \tag{66}$$

The dielectric susceptibility corresponding to the hkl Bragg reflection χ_{hkl} is given by

$$|\chi_{hkl}| = (\lambda^2/\pi r_e V) F_{hkl}. \tag{67}$$

In equation (65), J_0 is the spherical Bessel function of zero order which, in its

asymptotic form, becomes

$$\sin^2(\pi l \Delta_0^{-1} + \tfrac{1}{4}\pi).$$

The period of the standing wave pattern is therefore related to the geometric structure factor.

Of the many measurements of the geometric structure factor the most accurate is that by Aldred and Hart (1973). The material on which they worked was silicon, the material most readily manufactured as a perfect single crystal. If crystalline defects exist the periodicity of the Pendellösung fringes is modified.

Extremely precise measurements have been made of the geometric structure factor for a large number of Bragg reflections, from which the atomic scattering factors f_{hkl} have been deduced. Price *et al.* (1978) have used a refinement technique to evaluate from this data values of the anomalous dispersion corrections. The data, however, are for $f(\omega, g_{hkl})$, and like the other techniques the refinement procedure assumes no angular dependence of $f'(\omega, g_{hkl})$ and $f''(\omega, g_{hkl})$. In addition the Pendellösung technique can be used only when large perfect strain-free crystals are available. This limits its usefulness to the study of relatively few materials.

(e) Future developments

In recent times the technique for manufacturing 'crystals' using the vacuum deposition of alternating layers of elements having significantly different scattering powers has advanced to a stage where devices which can operate effectively at low photon energies have been fabricated. Henke *et al.* (1982) have discussed the performance of this class of reflector. The manufacturing skills developed by Barbee (1981) has enabled the construction of a Fabry–Perot etalon capable of operating in the soft X-ray region. In principle the refractive index of the spacer material between the elements of such an etalon can be measured to very high precision. The real problem with this method at present lies in the difficulty of producing layers with a homogeniety commensurate with the potential resolution of the etalon. If the manufacturing difficulties can be resolved this technique could yield results in a region of the X-ray spectrum for which results have been extraordinarily difficult to obtain.

4. Discussion

In this section discussion will centre on theoretical and experimental results for materials for which the cohesive forces are metallic, represented by copper and nickel, covalent represented by silicon, and ionic, represented by lithium fluoride.

(a) Experiments Close to an Absorption Edge: Copper and Nickel

The availability of synchrotron radiation sources has increased greatly the possibility of performing experiments to measure the anomalous dispersion corrections. Experiments to determine $f'(\omega, 0)$ and $f''(\omega, 0)$ for a range of wavelengths encompassing an absorption edge have been undertaken at both the SRC facility at Daresbury (U.K.), HASYLAB at the DESY facility (West Germany), the 'photon factory' (Japan), and SPEAR the Stanford (U.S.A.) facility. These experiments for the most part have been performed on thin (<10 μm) foils, usually belonging to the transition metal sequence. Experiments have been performed on a range of other elements, amongst them platinum, gold, zirconium, tantalum and tungsten.

In Fig. 9*a* the record of an experiment to determine $f'(\omega, 0)$ for copper using an X-ray interferometer is shown schematically. At the low energy side of the edge there is a smooth decrease of $f'(\omega, 0)$ until a minimum value is reached at the absorption edge. A slight increase occurs before a subsidiary minimum is reached about 15 eV above the energy of the absorption edge. Modulations are observed on the $f'(\omega, 0)$ curve, and these tend to become less significant as the energy of the incident photon increases. The experimental error claimed, on the scale of the diagram, is typically three times the width of the line. For comparison the values of $f'(\omega, 0)$ calculated using an approach similar to Cromer and Liberman (1970, 1981), which is valid only for free atoms, is shown in Fig. 9*a* as the dashed curve. Note the significant discrepancy between theory and experiment, which is a consequence of the interference of the ejected photoelectron with the electrons in its immediate vicinity. The energy range over which this modulation persists depends on temperature, the effect being more pronounced at low temperatures.

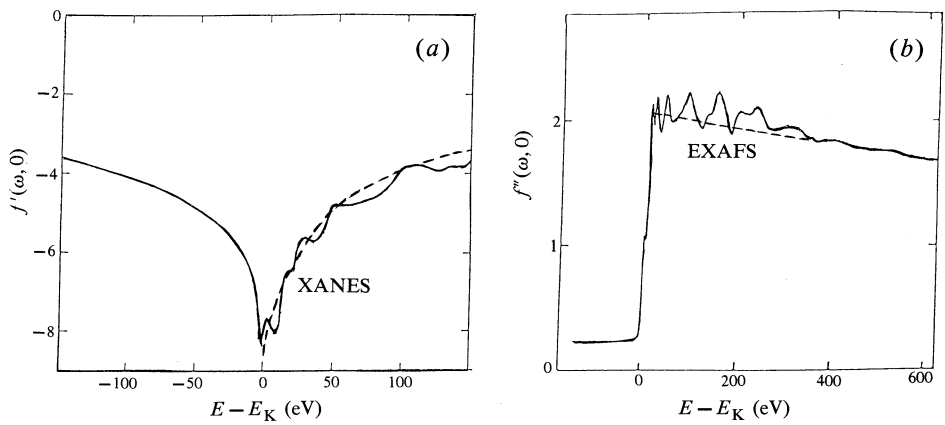

Fig. 9. (*a*) Variation of $f'(\omega, 0)$ in the region of the copper absorption edge showing XANES structure. (*b*) Kramers–Kronig transformation of (*a*) over an extended energy range showing both XANES and EXAFS regions. The dashed curves in each case are the results of calculations using the Cromer and Liberman (1970, 1981) program.

In the nonrelativistic theory $f'(\omega, 0)$ and $f''(\omega, 0)$ are related by the Kramers–Kronig transformation

$$f'(E_i, 0) = \frac{2}{\pi} \mathrm{P} \int \frac{E f''(E, 0)}{E^2 - E_i^2} \, \mathrm{d}E, \tag{68}$$

$$f''(E_i, 0) = \frac{2}{\pi} E_i \mathrm{P} \int \frac{f'(E, 0)}{E^2 - E_i^2} \, \mathrm{d}E. \tag{69}$$

Fig. 9*b* shows the Kramers–Kronig transform of the curve displayed in Fig. 9*a*. This exhibits the same modulations as those observed in linear attenuation measurements, both in the region of the edge (XANES) and away from it (EXAFS). Further, it shows the usual tendency for the averaged slope to be higher near the edge than would be expected from the extrapolation of photoelectric attenuation data taken at energies significantly greater than the edge energy. These values calculated using the Cromer and Liberman (1970, 1981) theory are shown in Fig. 9*b* as the dashed curve.

The fact that both $f'(\omega, 0)$ and $f''(\omega, 0)$ show EXAFS and XANES modulations is a consequence of the fact that in a real crystal the photoelectrons ejected from the atom by the incident beam interact with the electrons in neighbouring atoms. The theory of EXAFS is reasonably well developed (see e.g. Lee *et al.* 1981) but there still exist some problems in the formation of a fully quantitative theory. Nevertheless, the existing theories explain quite satisfactorily the shape of the $\mu_l(\omega)$ versus ω curve but, although the maxima and minima of the modulations occur where the theory predicts, their magnitudes may differ somewhat from the theoretical predictions.

Difficulties still exist in the near edge region but the multiple scattering theory described by Durham (1983) provides some hope that a proper explanation for XANES will be found soon.

Fig. 9 demonstrates the general features exhibited by the X-ray interferometer experiments of Siddons and Hart (1983), Bonse *et al.* (1983) and Bonse and Hartmann-Lotsch (1984). These same general features occur in the results of X-ray attenuation experiments. These range from the EXAFS-type experiments of Dreier *et al.* (1984) to X-ray interferometer beam contrast experiments made by Bonse and Hartmann-Lotsch (1984). Measurements made by Fukamachi *et al.* (1978) using the Kramers–Kronig transform and the critical angle technique exhibit similar features.

Table 1. Comparison of $f'(\omega_K, 0)$ for Cu and Ni

Here KK implies that a Kramers–Kronig transformation has been used to transform scattering cross section data into $f'(\omega_K, 0)$. The experimental errors claimed are not worse than 5%

Reference	Method	$f'(\omega, 0)$ Cu	Ni
Experiment			
Freund (1975)	Bragg reflection	−8·2	
Bonse & Materlik (1976)	Interferometer		−8·1
Bonse *et al* (1983)	Interferometer	−8·3	
Siddons & Hart (1983)	Interferometer	−9·3	−9·2
Kawamura & Fukamachi (1978)	KK		−7·9
Fukamachi *et al.* (1978)	KK	−8·8	
	Critical angle	−10·0	
Dreier *et al.* (1984)	KK	−8·2	−7·8
Bonse & Hartmann-Lotsch (1984)	Interferometer	−8·3	−8·1
	KK	−8·3	−7·7
Theory			
Cromer & Liberman (1970, 1981)		−10·5	−9·0

Within each experimental data set reproducibility and self-consistency are very good. Typical claims as to experimental precision range from 2% in the case of Siddons and Hart (1983) to 5% for Dreier *et al.* (1984). Remote from the absorption edge all the experimental results are in good agreement with one another and, indeed, with the calculations by Cromer and Liberman (1970, 1981). But near the edge, where multiple scattering of the ejected photoelectrons occurs, significant differences occur between the different experimental data sets and the theoretical values. Hart and Siddons (1981), using a slightly modified Cromer and Liberman program, found that the theoretical curve predicts the trend of $f'(\omega, 0)$ as a function of ω extremely well.

Very significant discrepancies exist between these experiments, which can be illustrated by the results of experiments performed at the K-absorption edge of copper and nickel, and which are set out in Table 1. It would seem that the consensus value for copper is $-8\cdot3$ electrons, with no fewer than five measurements lying within 1% of this value. However, the theoretical (albeit free atom) value is $-10\cdot5$ electrons and three measurements lie in the range $-8\cdot3$ to $-10\cdot5$ electrons.

The agreement between experiments is not quite so good for the case of nickel, but all except the Siddons and Hart (1983) value lie in the range $-7\cdot7$ to $-8\cdot1$ electrons, which is within the claimed accuracy for most experiments. However, the theoretical value is $-9\cdot0$ electrons which lies much closer to the Siddons and Hart value than the others. Given the excellent agreement which exists between theory and experiment at energies remote from the edge and the fact that theory successfully predicts the trend of the $f'(\omega, 0)$ versus ω curve, the differences in $f'(\omega_K, 0)$ are somewhat puzzling.

Of the results shown in Table 1 only the X-ray interferometers provide direct measurements of $f'(\omega_K, 0)$; all the others determine it indirectly. In the experiment performed by Freund (1975) numerous corrections had to be made, not the least of which was the correction for thermal diffuse and Compton scattering, and it was also necessary to measure the linear attenuation coefficient μ_l. In the event his experimental results for μ_l do not show EXAFS and are not in accord with the more recent measurements by Dreier *et al.* (1984). Also, because Freund measured $f'(\omega_K, g_{222})$ and not $f'(\omega_K, 0)$, the inclusion of his results in Table 1 is only warranted if there is no angular dependence of the real part of the anomalous dispersion correction on scattering angle.

Kramers–Kronig transformations are extremely difficult to perform. It is necessary to have precise measurements of the linear attenuation coefficient over a wide energy range. In the case of Dreier *et al.* (1984), recourse was made to the data presented by McMaster *et al.* (1969) and this data set is known (Creagh and Hubbell 1985) to contain a significant systematic error. This must cast some doubt on the validity of their estimate of $f'(\omega_K, 0)$. Similar remarks can be made about the experiments by Kawamura and Fukamachi (1978) and Fukamachi *et al.* (1978). Further, all Kramers–Kronig calculations are subject to a systematic error because of the neglect of the K-shell linewidth in the calculation. This effect of the neglect of this parameter is most significant in the region of the edge.

The critical angle experiment by Fukamachi *et al.* (1978) is made at a fixed (nonzero) angle of scattering and can be included in Table 1 only if no angular dependence of the real part of the anomalous dispersion correction exists.

The origin of the discrepancy between the X-ray interferometer measurements is difficult to assess. The interferometers themselves are quite differently constructed and are mounted at quite different synchrotron radiation sources. It is known (M. Hart, personal communication 1982) that the results taken using the Ångström ruler interferometer at LURE, DESY, SRS Daresbury, and in Hart's laboratory are self-consistent. No similar information exists for Bonse's interferometer. It seems likely that the source of the discrepancy lies in the energy resolution of the interferometers. Although, in the first instance this is determined by the width of the Laue case rocking curve for the interferometer, it is considerably broadened by thermal fluctuations and mechanical vibrations. The effect of degradation in energy resolution is the reduction in the amplitude of the EXAFS and XANES and the increase in the value of $f'(\omega_K, 0)$. This effect can be readily seen by comparing the work of Bonse and Materlik (1975)

with that of Bonse and Hartmann-Lotsch (1984). The interferometer configurations are identical yet the earlier work barely shows the effect of EXAFS, in contrast to the later work. The difference is predominantly that the early experiment was done at a work-station to which the interferometer had to be taken and mounted for each experimental run. For the latter, the interferometer has had a permanent mounting on the beam line of the synchrotron, and the mechanical and thermal stability of the system has therefore been improved significantly.

That neither of the interferometer experiments accord with theory is not surprising given that the theory has been developed for a free atom system in which no change in polarization is envisaged. Also the theory itself does not make adequate provision for such problems as multiple ionization of the K shell and the effect of finite lifetime in the excited state. Recent comments by Stearns (1984) concerning the broadening of EXAFS spectra tend to support the notion that the explanation of the discrepancy between theory and experiment lies partly in the failure of theory to describe adequately the photon–atom interaction under conditions of high photon flux. The discrepancy between experiments might well arise from differences in parameters such as energy resolution, source stability and source brilliance.

Until some of the theoretical and experimental problems are resolved the correct value of $f'(\omega_K, 0)$ will remain uncertain. However, as mentioned earlier, the measured values of $f'(\omega, 0)$ remote from the edge are in good agreement with the values computed using the Cromer and Liberman (1970, 1981) program.

(b) Experiments Remote from an Absorption Edge

Since 1960 a number of experiments have been performed using characteristic radiation from conventional laboratory X-ray sources. Since most crystallographic crystal structure analyses are made in laboratories which use conventional sealed-tube X-ray sources this forms a very important set of results. To date most of the research has centred on the alkali and alkaline-earth halides and the semiconductor crystals silicon and germanium.

Here we discuss the measurements made in a typical ionically bonded crystal, lithium fluoride, and the covalently bound crystal, silicon. The refractive index of lithium fluoride has been measured by Creagh (1970), Creagh and Hart (1970), Bonse and Hellkötter (1969) and Creagh (1984) using X-ray interferometer techniques. It has also been measured by Deutsch and Hart (1984) using the deviation of a prism technique. Measurements were made at the characteristic K-photon energies from copper, molybdenum and silver sealed X-ray tubes. From these measurements values of $f'(\omega, 0)$ were deduced.

Using X-ray attenuation measurements Creagh (1975, 1978, 1980) has determined $f'(\omega, 0)$ for a range of alkali and alkaline-earth halides. Gerward *et al.* (1979) have used a similar method to determine $f'(\omega, 0)$ as a function of photon energy for silicon.

Data for lithium fluoride and silicon are included in Table 2 together with the results of the deformation density study by Price *et al.* (1978), who used the Pendellösung measurements for silicon reported by Aldred and Hart (1973). We note that the inclusion of these results in the table is valid only if it can be assumed that there is no functional dependence of $f'(\omega, \boldsymbol{\Delta})$ on $\boldsymbol{\Delta}$. Although quite good agreement exists between the experimental results significant differences are found with the calculations of Cromer and Liberman (1970) and Wagenfeld (1975). This is quite unexpected and,

as Creagh (1984) has shown, all the low atomic number elements he has studied follow the same pattern. If the ratio $(f'_{\text{exp}}-f'_{\text{CL}})/f'_{\text{CL}}$ is plotted as a function of the parameter $\lambda/\lambda_{\text{K}}$, where f'_{exp} is the experimental value and f'_{CL} is the value from Cromer and Liberman (1970), then:

(i) the experimental results are greater than the theory predicts for $\lambda/\lambda_{\text{K}} < 0{\cdot}25$;

(ii) the experimental results are less than the theory predicts for $\lambda/\lambda_{\text{K}} > 0{\cdot}25$. This difference tends to zero as λ tends to λ_{K}, in accord with the observations made by synchrotron radiation users to the effect that, in general, on approaching the edge the predictions of Cromer and Liberman (1970, 1981) are in good agreement with experiment.

Table 2. Comparison of measurements of $f'(\omega, 0)$ for LiF and Si at the characteristic K-shell radiations of molybdenum and silver

The experimental accuracy (in %) claimed by respective authors is given in parentheses

Sample	Reference	$f'(\omega,0)$ Mo Kα_1	Ag Kα_1
LiF	*Theory*		
	Cromer & Liberman (1970)	0·014	0·006
	Wagenfeld (1975)	0·023	0·015
	Experiment		
	Creagh (1984)	0·020 (10)	0·014 (10)
	Deutsch & Hart (1984)	0·0217(1)	0·0133(1)
Si	*Theory*		
	Cromer & Liberman (1970)	0·071	0·042
	Wagenfeld (1975)	0·101	0·071
	Experiment		
	Cusatis & Hart (1975)	0·0863(2)	0·0568(2)
	Price *et al.* (1978)	0·085 (7)	0·047 (7)
	Gerward *et al.* (1979)	0·099 (7)	0·070 (7)
	Creagh (1984)	0·091 (5)	0·060 (5)
	Deutsch & Hart (1984)	0·0847(1)	0·0537(1)

We note in Table 2 that the nonrelativistic approach used by Wagenfeld (1975, 1985) also is not in agreement with the observed values. This has been attributed by Deutsch and Hart (1984) to a failure to account properly for the effect of higher electron shells in the calculations. Also the experimental evidence tends to support the contention of Parker and Pratt (1982) that there is no angular dependence in $f'(\omega, \boldsymbol{\Delta})$, in contradiction with Wagenfeld's (1975) theory. The experimental values lie between the values calculated using the relativistic and the nonrelativistic theory. However, the relativistic theory gives a better description of photon scattering as the incident photon energy approaches the absorption edge energy. In this case the value of the integral in equation (44) is much larger than the terms due to the total kinetic energy of the atom:

$$\tfrac{5}{3}E_{\text{tot}}/mc^2-\tfrac{1}{2}Z(\hbar\omega/mc^2)^2\,.$$

In the high energy limit, however, these latter terms dominate the expression for $f'(\omega, 0)$. It would appear therefore that the source of error lies in the calculation of

E_{tot} for a bound system. The electronic energy levels for atoms bound into crystals must be different from those for free atoms.

Some attempts have been made to estimate the scattering cross sections for crystalline materials using band-theory calculations. Indeed Takama and Sato (1982) reported good agreement between their Pendellösung measurements on copper and the band-theory calculations of Wakoh and Yamashita (1971). Such comparisons are possible only for those simple crystal structures for which the positional parameters are well known.

Until some technique for estimating E_{tot} for bound atomic systems is established, difficulties will be experienced in comparing theoretical and experimental values for $f'(\omega, 0)$ in the high energy limit ($\omega \rightarrow \infty$). This is of some significance since, for elements with low atomic numbers, measurements which are made with the characteristic emissions from sealed X-ray tubes are made effectively in the high energy limit ($\omega \gg \omega_K$). A solution to this problem should be sought as a matter of some urgency.

Acknowledgments

It is my pleasure to acknowledge the encouragement and support given to me by Dr A. McL. (Sandy) Mathieson in the many years during which we have been friends. I wish him a most enjoyable retirement from the CSIRO. I must also acknowledge the support of the Australian Research Grants Scheme which has in part funded my research.

References

Akhiezer, A. J., and Berestetskii, V. B. (1957). 'Quantum Electrodynamics' (Oak Ridge Lab.: Tennessee).

Aldred, P. J. E., and Hart, M. (1973). *Proc. R. Soc. London* A **332**, 223–8; 239–54.

Barbee, T. W. (1981). Proc. Cont. on Low Energy X-ray Diagnostics (Eds D. T. Attwood, H. C. Woolfe and B. L. Henke), pp. 101–21 (AIP: New York).

Barnea, Z. (1975). *In* 'Anomalous Scattering' (Eds S. Ramaseshan and S. C. Abrahams), pp. 289–91 (Munksgaard: Copenhagen).

Bearden, J. A. (1931). *Phys. Rev.* **38**, 835.

Bearden, J. A. (1932). *Phys. Rev.* **39**, 1.

Bethe, H. A., and Salpeter, E. E. (1957). *In* 'Encyclopaedia of Physics', Vol. 35 (Ed. S. Flugge) (Springer: Berlin).

Bijvoet, J. M. (1951). *In* 'Computing Methods and the Phase Problem in X-ray Crystallography' (Ed. R. Pepinski), pp. 84–8 (Pennsylvania State College).

Bijvoet, J. M., Peerdeman, A. F., and Van Bommel, A. J. (1951). *Nature* **168**, 271.

Bonse, U., and Hart, M. (1965). *Appl. Phys. Lett.* **7**, 238–42.

Bonse, U., and Hart, M. (1966). *Z. Phys.* **189**, 151–65.

Bonse, U., and Hartmann-Lotsch, I. (1984). *Nucl. Instrum. Methods* **222**, 185–8.

Bonse, U., Hartmann-Lotsch, I., and Lotsch, H. (1983). *In* 'EXAFS and Near Edge Structures', Vol. 27 (Eds A. Bianconi *et al.*), pp. 376–7 (Springer: Berlin).

Bonse, U., and Hellkötter, H. (1969). *Z. Phys.* **223**, 345–52.

Bonse, U., and Materlik, G. (1972). *Z. Phys.* **253**, 232–9.

Bonse, U., and Materlik, G. (1975). *In* 'Anomalous Scattering' (Eds S. Ramaseshan and S. C. Abrahams), pp. 107–9 (Munksgaard: Copenhagen).

Bonse, U., and Materlik, G. (1976). *Z. Phys.* B **23**, 189–91.

Bonse, U., Spieker, P., Hein, J. Th., and Materlik, G. (1980). *Nucl. Instrum. Methods* **172**, 223–6.

Brysk, H., and Zerby, C. D. (1968). *Phys. Rev.* **171**, 292–8.

Cole, H., and Stemple, N. R. (1962). *J. Appl. Phys.* **33**, 2227–33.

Compton, A. H. (1923). *Philos. Mag.* **45**, 1121–31.

Creagh, D. C. (1968). M.Sc. Thesis, University of Bristol.
Creagh, D. C. (1970). *Aust. J. Phys.* **23**, 99–103.
Creagh, D. C. (1975). *Aust. J. Phys.* **28**, 543–55.
Creagh, D. C. (1977). *Phys. Status Solidi (a)* **39**, 705–15.
Creagh, D. C. (1978). *In* 'Advances in X-ray Analysis', Vol. 21 (Eds C. S. Barrett and D. E. Leyden), pp. 149–53 (Plenum: New York).
Creagh, D. C. (1980). *Phys. Lett.* A **77**, 129–32.
Creagh, D. C. (1984). *Phys. Lett.* A **103**, 52–6.
Creagh, D. C., and Hart, M. (1970). *Phys. Status Solidi* **37**, 753–8.
Creagh, D. C., and Hubbell, J. H. (1985). *Acta Crystallogr.* B (in press).
Cromer, D. T. (1965). *Acta Crystallogr.* **18**, 17–23.
Cromer, D. T., and Liberman, D. (1970). *J. Chem. Phys.* **53**, 1891–8.
Cromer, D. T., and Liberman, D. (1981). *Acta Crystallogr.* A **37**, 267.
Cusatis, C., and Hart, M. (1975). *In* 'Anomalous Scattering' (Eds S. Ramaseshan and S. C. Abrahams), pp. 57–67 (Munksgaard: Copenhagen).
Deutsch, M., and Hart, M. (1984). *Phys. Rev.* B **30**, 640–2; 643–6.
Dreier, P., Rabe, P., Matzfeldt, W., and Niemann, W. (1984). *J. Phys.* C **17**, 3123–36.
Duane, W., and Patterson, R. A. (1920). *Phys. Rev.* **16**, 532.
Durham, P. J. (1983). *In* 'EXAFS and Near Edge Structure' (Eds A. Bianconi *et al.*), pp. 37–43 (Springer: Berlin).
Eisenlohr, H., and Muller, G. L. (1954). *Z. Phys.* **136**, 491–510; 511–33.
Ewald, P. P. (1916). *Ann. Phys. (Leipzig)* **49**, 1–38; 117–43.
Freund, A. (1975). *In* 'Anomalous Scattering' (Eds S. Ramaseshan and S. C. Abrahams), pp. 69–86 (Munksgaard: Copenhagen).
Fukamachi, R., and Hosoya, S. (1975). *Acta Crystallogr.* A **31**, 215–20.
Fukamachi, T., Hosoya, S., Kawamura, T., and Hastings, J. (1977). *J. Appl. Crystallogr.* **10**, 321–4.
Fukamachi, T., Hosoya, S., Kawamura, T., Hunter, S., and Nakano, Y. (1978). *J. Appl. Phys. (Japan)* **17–2**, 326–8.
Fuoss, P. H. (1980). Ph.D. Dissertation, Stanford University.
Fuoss, P., and Bienenstock, A. (1981). *In* 'Inner-shell and X-ray Physics of Atoms and Solids' (Eds D. J. Fabian *et al.*), pp. 875–84 (Plenum: New York).
Fuoss, P. H., Warburton, W. K., and Bienenstock, A. (1981). *J. Non-Cryst. Solids* **35–6**, 1233.
Gavrila, M. (1981). *In* 'Inner–shell Processes' (Ed. B. Craseman), pp. 357–88 (Plenum: New York).
Gell-Mann, M., Goldberger, M. L., and Thirring, W. (1956). *Phys. Rev.* **95**, 1612.
Gerward, L., Theusen, G., Stibius-Jensen, M., and Alstrup, I. (1979). *Acta Crystallogr.* A **35**, 852–7.
Goldberger, M. L., and Watson, K. L. (1965). 'Collision Theory' (Wiley: New York).
Grodstein, G. W. (1957). NBS Circular No. 583 (U.S. Dept. of Commerce: Washington).
Hart, M. (1968). *J. Phys.* D **1**, 1405–8.
Hart, M., and Siddons, D. P. (1981). *Proc. R. Soc. London* A **376**, 465–82.
Hayward, E., Barber, W. C., and McCarthy, J. J. (1974). *Phys. Rev.* C **10**, 3562.
Henke, B. L., Lee, P., Tanaka, T. J., Shimabukuro, R. L., and Fujikawa, B. K. (1982). *At. Data Nucl. Data Tables* **27**, 1–144.
Hjalmar, E. (1920). *Z. Phys.* **1**, 439.
Hönl, H. (1933*a*). *Z. Phys.* **84**, 1–16.
Hönl, H. (1933*b*). *Ann. Phys. (Leipzig)* **18**, 625–57.
Hosoya, S. (1975). *In* 'Anomalous Scattering' (Eds S. Ramaseshan and S. C. Abrahams), pp. 275–87 (Munksgaard: Copenhagen).
Ibers, J. A., and Hamilton, W. C. (Eds) (1974). 'International Tables for X-ray Crystallography', Vol. 4 (Kynoch: Birmingham).
James, R. W. (1955). 'The Optical Principles of the Diffraction of X-ray' (Cornell Univ. Press).
Kato, N. (1960). *Acta Crystallogr.* **13**, 349–56.
Kato, N. (1961). *Acta Crystallogr.* **14**, 526–32; 627–36.
Kato, N., and Lang, A. R. (1959). *Acta Crystallogr.* **12**, 787.
Kawamura, T., and Fukamachi, T. (1978). *J. Appl. Phys. Jpn* **17**, 224.

Kissel, L., and Pratt, R. H. (1983). *In* 'Atomic Inner-shell Physics' (Ed. B. Craseman) (Plenum: New York).
Kissel, L., Pratt, R. H., and Roy, S. C. (1980). *Phys. Rev.* A **22**, 1970–2204.
Kohn, W., and Sham, L. J. (1965). *Phys. Rev.* **140**, 1133–2004.
Larsson, A., Siegbahn, M., and Waller, I. (1924). *Naturwissenschaften* **12**, 1212.
Lee, P. A., Citrin, P. H., Eisenberger, P., and Kindaid, B. M. (1981). *Rev. Mod. Phys.* **53**, 769.
McMaster, W. H., Del Grande, N., Mallett, J. H., and Hubbell, J. H. (1969). Lawrence Livermore Laboratory Rep. UCRL-50174-SEC2-R1.
Mizushima, M. (1970). 'Quantum Mechanics of Atomic Spectra and Atomic Structure' (Benjamin: New York).
Papatzacos, P., and Mork, K. (1975). *Phys. Rep.* **21**, 81–118.
Parker, J. C., and Pratt, R. H. (1982). Univ. of Pittsburgh Rep. No. PITT-286.
Parratt, L. G., and Hempstead, C. F. (1954). *Phys. Rev.* **94**, 1593–1609.
Phillips, J. C., and Hodgson, K. O. (1980*a*). *Acta Crystallogr.* A **36**, 856–64.
Phillips, J. C., and Hodgson, K. O. (1980*b*). *In* 'Synchrotron Radiation Research' (Eds H. Winnick and S. Doniach), pp. 565–604 (Plenum: New York).
Phillips, J. C., Templeton, D. H., Templeton, J. C., and Hodgson, K. O. (1978). *Science* **201**, 257–9.
Post, B. (1975). *In* 'Anomalous Scattering' (Eds S. Ramaseshan and S. C. Abrahams), pp. 85–91 (Munksgaard: Copenhagen).
Price, P. F., Maslen, E. N., and Mair, S. L. (1978). *Acta Crystallogr.* A **34**, 183–93.
Sakurai, M. (1967). 'Advanced Quantum Mechanics' (Addison–Wesley: New York).
Scofield, J. (1973). Lawrence Livermore Rep. No. UCRL-51326.
Senström, W. (1919). Dissertation, University of Lund.
Siddons, D. P., and Hart, M. (1983). *In* 'EXAFS and Near Edge Structure' (Eds A. Bianconi *et al.*), pp. 373–5 (Springer: Berlin).
Slater, J. C. (1951). *Phys. Rev.* **81**, 389.
Stearns, D. G. (1984). *Philos. Mag.* B **49**, 541–58.
Stibius-Jensen, M. (1979). *Phys. Lett.* A **74**, 41–4.
Storm, E., and Israel, H. (1970). *Nucl. Data Tables* A **7**, 565.
Stout, G. H., and Jensen, L. H. (1968). 'X-ray Structure Determination: A Practical Guide' (Macmillan: New York).
Suguira, Y. (1927). *J. Phys. (Paris)* **8**, 113–24.
Takama, T., and Sato, S. (1982). *Philos. Mag.* B **45**, 615–26.
Templeton, L. K., and Templeton, D. O. (1978). *Acta Crystallogr.* A **34**, 368–73.
Templeton, L. K., and Templeton, D. O. (1985). *Acta Crystallogr.* (in press).
Templeton, D. O., Templeton, L. K., Philips, J. C., and Hodgson, K. O. (1980). *Acta Crystallogr.* A **36**, 436.
Wagenfeld, H. (1966). *Phys. Rev.* **144**, 236.
Wagenfeld, H. (1975). *In* 'Anomalous Scattering' (Eds S. Ramaseshan and S. C. Abrahams), pp. 12–23 (Munksgaard: Copenhagen).
Wagenfeld, H. (1985). *Acta Crystallogr.* (in press).
Wakoh, S., and Yamashita, J. (1971). *J. Phys. Soc. Jpn* **30**, 422.
Waller, I. (1927). *Z. Phys.* **51**, 213.
Warren, B. E. (1969). 'X-ray Diffraction' (Addison–Wesley: London).
Zachariasen, W. H. (1945). 'Theory of X-ray Diffraction in Crystals' (Dover: New York).

Manuscript received 3 January, accepted 24 April 1985